

Customer : Space ConneXions Ltd acting for Defra	Document Ref : ISAR-DEFRA-FREP02 Issue Date : 17 June 2008 Issue : 1
--	---

Title : **Validation of AATSR Sea Surface Temperature Products using the ship borne ISAR Radiometer - Phase 2 Final Report**

Abstract : This document reports work performed on the contract to validate AATSR SST products using the ISAR shipboard radiometer. It summarises four years of validation results and describes the specific achievements from Phase 2

Authors :

Ian Robinson,
Werenfrid Wimmer

Distribution : Hugh Kelliher, Space ConneXions Ltd
Dr Craig Donlon, UK Met Office
AATSR Validation Scientist, Dr. Gary Corlett, Uni. Leicester

© The Copyright of this document is the property of National Oceanography Centre, Southampton. It is supplied on the express terms that it be treated as confidential, and may not be copied, or disclosed, to any third party, unless authorised by NOCS in writing.

National Oceanography Centre, Southampton
European Way, Southampton, SO14 3ZH, UK
Tel: +44 (0)23 8059 3438
Fax: +44 (0)23 8059 3059

Executive Summary.....	4
1. Introduction.....	6
2. The ISAR System.....	8
2.1 The need for autonomous radiometers on ships of opportunity.....	8
2.2 The ISAR instrument.....	9
2.3 Operational deployment of ISAR.....	12
2.4 Calibration and validation of the ISAR instrument.....	14
2.5 ISAR Performance.....	15
3. Measurements made by the ISAR System.....	17
3.1 Data collected from ISAR deployments.....	17
3.2 The variability of skin SST in the Bay of Biscay.....	21
3.3 Match-ups between ISAR and AATSR samples.....	24
4. Validation of AATSR against ISAR data.....	28
4.1 Dual view algorithms.....	28
4.2 Nadir-view only algorithms.....	34
4.3 Comparison between the performance of the different algorithms.....	38
5. Ancillary Studies.....	42
5.1 A quality flagging scheme for validation match-ups.....	42
5.2 Study of skin-bulk processes.....	46
6. Conclusion.....	48
6.1 Achievements of the project.....	48
6.2 Requirement for ongoing work.....	48
Appendix A Revised internal calibration algorithm.....	50
Appendix B Data acquired by ISAR.....	53
B.1 Data records for D10: ISAR-002, 21 February to 10 May 2006.....	53
B.2 Data records for D11: ISAR-003, 10 May to 9 August 2006.....	54
B.3 Data records for D12: ISAR-002, 9 August to 6 November 2006.....	55
B.4 Data records for D13: ISAR-003, 6 December 2006 to 4 January 2007.....	56
B.5 Data records for D14: ISAR-002, 8 February to 8 May 2007.....	57
B.6 Data records for D15: ISAR-003, 8 May to 1 June 2007.....	58
B.7 Data records for D16: ISAR-002, 4 June to 24 August 2007.....	59
B.8 Data records for D17: ISAR-003, 24 August to 25 November 2007.....	60
B.9 Data records for D18: ISAR-003, 29 November 2007 to 7 January 2008.....	61
Appendix C Intercomparison tests for CASOTS-2 Blackbody.....	62
Appendix D Pre and post cruise validation data.....	64
D.1 Calibration plots for D10: ISAR-002, 21 February to 10 May 2006.....	64
D.2 Calibration plots for D11: ISAR-003, 10 May to 9 August 2006.....	65
D.3 Calibration plots for D12: ISAR-002, 9 August to 6 November 2006.....	66
D.4 Calibration plots for D13: ISAR-003, 6 December 2006 to 4 January 2007.....	67
D.5 Calibration plots for D14: ISAR-002, 8 February to 8 May 2007.....	68
D.6 Calibration plots for D15: ISAR-002, 4 June to 24 August 2007.....	68
D.7 Calibration plots for D16: ISAR-002, 4 June to 24 August 2007.....	69
D.8 Calibration plots for D17: ISAR-003, 24 August to 25 November 2007.....	70
D.9 Calibration plots for D18: ISAR-003, 29 November 2007 to 7 January 2008.....	71
Appendix E ISAR Instrument Service Logs.....	72
Appendix F Acronyms.....	74

AMENDMENT RECORD SHEET FOR THIS DOCUMENT

ISSUE-draft	DATE	REASON
0A	6 May 2008	Initial draft issue for discussion with Space ConneXions
1	17 June, 2008	Final version following comments by Space ConneXions

Executive Summary

Since March 2004, the National Oceanography Centre, Southampton has undertaken a programme of work to measure sea surface temperature (SST) at the level of the surface skin, in order to provide a set of baseline data for validating the skin-SST products retrieved from the Advanced Along-Track Scanning Radiometer (AATSR), a sensor procured by Defra and flown on ESA's Envisat satellite. The particular role of this subcontract within the wider AATSR validation programme is to provide a match-up dataset that monitors the ongoing stability of the AATSR performance.

This document reports on the achievements during Phase 2 of the project, between March 2006 and February 2008. It also reviews the full four years of data acquired from both Phase 1 and Phase 2, following reanalysis of the whole dataset.

The work is performed using a unique instrument, the Infrared SST Autonomous Radiometer (ISAR). An ISAR instrument, mounted on the bridge of the P&O ferry *Pride of Bilbao*, measures skin-SST every few minutes when there is no precipitation. Thus it observes SST in exactly the same way as the AATSR does. Operating autonomously day and night, it acquires *in situ* observations for comparison with the satellite data whenever the AATSR passes over the ferry in cloud-free conditions.

During the four years of the project so far a total of 1649 validation pairs of dual-view satellite retrievals and *in situ* observations were acquired, measured within 1 km and 2 hours of each other, corresponding to 130 different overpasses. Using a less strict criterion of coincidence, within 25 km and 6 hours, 7290 validation pairs were acquired from 230 overpasses. The matches confirm that over the region of the Bay of Biscay and English Channel the SST data produced from the AATSR dual view observations are very accurate and performing well within their specification. For the 2 hour and 1 km matches, the difference between the AATSR temperatures and the ship-based ISAR temperatures is 0.01 ± 0.30 °C for the 3-waveband algorithm (night time overpasses corresponding to about 59% of the matches) and -0.04 ± 0.44 °C for the 2-waveband algorithm (daytime, about 41% of matches), with no evident drift over the four years.

The match-up data acquired from ISAR deployments on *Pride of Bilbao* have made a major contribution to the inputs available to the AATSR Validation Scientist. They have been the only source of direct match-ups at temperatures lower than 15°C, and at present provide the only ongoing regular programme supplying validation data for AATSR. During the four years of this project, an increasing number of agencies have adopted AATSR SST products as a standard for bias correction of other satellite SST products, for use in generating high quality SST analyses for ocean forecasting and climate records. The ISAR data provide an essential underpinning to that key role.

During Phase 2 of the project, two ancillary studies were performed. In the first of these the differences between the ISAR skin SST and more conventional ship-based SST measurements were analysed. The conclusion was reached that using hull-mounted or engine intake thermometry as a proxy for the skin SST viewed by satellites leads to uncertainties that degrade the quality of satellite validation based on such data. The degradation is significant when validating a high specification sensor such as the AATSR.

The second ancillary study developed and applied a new methodology for assigning quality values to match-up pairs of satellite and in situ observations. These are based on criteria associated with how representative the in situ observation is of the SST in the satellite observation's field of view. The use of such objectively-derived quality values will in future assist the AATSR validation programme to better assign confidence values to relatively small populations of match-up data.

1. Introduction

In March 2006, the Department for Environment, Food and Rural Affairs (Defra) renewed a contract with the National Oceanography Centre, Southampton (NOCS) originally initiated in March 2004 through its managing agent, Space ConneXions Ltd. This commissioned a further two-year programme of work to measure sea surface temperature (SST) at the ocean surface skin, in order to provide a set of baseline data for validating the skin-SST products retrieved from the Advanced Along-Track Scanning Radiometer (AATSR). The AATSR is an Earth Observation sensor procured by Defra, presently operating on ESA's Envisat satellite, in order to provide a global record of SST of the highest quality and with an absolute accuracy that leads the world. Its primary objective is to supply reliable evidence about the Earth's changing climate as revealed by decadal trends in SST.

One of the essentials for achieving the desired stability and accuracy of global SST measurements, in addition to the fundamental design of the AATSR instrument itself, is to be able to confirm the quality of its measurements by independent observations made at sea level. This requirement is met by the AATSR validation programme that is supported by Defra through the Data Exploitation Contract and coordinated by the AATSR Validation Scientist. The particular role of the NOCS subcontract within the wider AATSR validation programme is to provide a match-up dataset of coincident AATSR and ship-based radiometer measurements of the sea surface skin temperature. In order to be able to monitor the ongoing stability of the AATSR performance, the acquisition of matching *in situ* data must be sustained by repeatedly sampling transects across the same region of sea over the AATSR's lifetime.

This goal has been achieved by deploying the Infrared SST Autonomous Radiometer (ISAR), a unique instrument designed by Dr Craig Donlon¹ to measure skin SST to within ± 0.1 K from ships of opportunity without operator supervision. Two ISARs constructed at NOCS were made available for the AATSR validation work. One of these at a time is mounted on the upper bridge of the P&O ferry *Pride of Bilbao*, which makes regular crossings of the Bay of Biscay and English Channel. The ISAR measures skin-SST every few minutes when there is no precipitation, observing the sea surface in exactly the same way as the AATSR does. Because it operates autonomously day and night, ISAR can acquire *in situ* observations to match the satellite data whenever the AATSR passes over the ferry in cloud-free conditions.

¹ See the following recent scientific publication: Donlon C, Robinson I S, Reynolds M, Wimmer W, Fisher G, Edwards R, Nightingale T J An Infrared Sea Surface Temperature Autonomous Radiometer (ISAR) for Deployment aboard Volunteer Observing Ships (VOS). *Journal of Atmospheric and Oceanic Technology* **25** (1): 93-113, 2008.

During the four years of the project so far, well over 1000 matched pairs of dual-view satellite retrievals and *in situ* observations have been acquired for validation, along with a suite of ancillary measurements including the SST measured by conventional (sub-surface) thermometry, meteorological parameters and radiative heat fluxes. The analysis of the matched pairs of *in situ* and AATSR-derived skin SST have shown close agreement to better than 0.1 K with the dual-view SST retrievals from the AATSR, while confirming the evidence from other validation experiments that the nadir-only SST retrievals during the daytime, when only 2 channels can be used, display a warm bias of about 0.5 K. The ISAR system has proved its ability to deliver regular match-ups against satellite data throughout the year, at a rate which far exceeds the occasional measurements hitherto made by manned radiometers on research cruises. During Phase 2 its performance has been improved by the adoption of new SST retrieval software.

This document provides a Phase 2 final report which not only describes the activities and achievements of the second phase of the ISAR-AATSR validation contract from 2006 to 2008 but also summarises the complete set of validation matches for AATSR over the four years the contract has been running so far. Section 2 briefly describes the ISAR measurement system, and minor changes made in Phase 2, although a more complete description and appraisal of its suitability for validation work can be found in the Final report of Phase 1 of the Project². Section 3 presents the results that were obtained during 2006 and 2007 in terms of the ISAR performance and the number of matches obtained with AATSR data. Section 4 examines what the matches with ISAR have revealed about the quality of the AATSR SST data products during the full period from 2004 to 2008.

Section 5 summarises the outcomes of two ancillary studies performed as part of Phase 2. The first analysed the capacity for conventional SST measurements using hull thermometry to serve as an effective proxy for skin temperature measurements when validating satellite SST. The second explored the quality of individual matched pairs in terms of how representative the skin SST point sample from ISAR is of the 1 km² area average of SST measured by AATSR. It led to the definition of quality values assigned to each match-up pair. Separate reports have been produced for each of these ancillary studies.

Section 6 draws broad conclusions about what the project has achieved and points towards the ongoing work that is required to maintain confidence in the validity of AATSR data products. The Appendices contain detailed tables defining the data acquired during the project, maps of match-up locations and figures displaying the data graphically.

² Robinson, I. S., Wimmer, W. and Donlon, C. J., 2006. *Validation of AATSR Sea Surface Temperature Products using the shipborne ISAR Radiometer - Final Report* National Oceanography Centre Report to DEFRA, Document reference "ISAR-DEFRA-FREP01", March 2006, 39pp plus appendices.

2. The ISAR System

2.1 The need for autonomous radiometers on ships of opportunity

Two requirements dictate the design of the ship-borne radiometer; the ability to measure the skin temperature of the ocean and the capacity for autonomous operation. Both of these are needed to provide an effective validation programme for a satellite sensor intended (as is the AATSR) to deliver skin SST data products specified to an accuracy of better than ± 0.3 K.

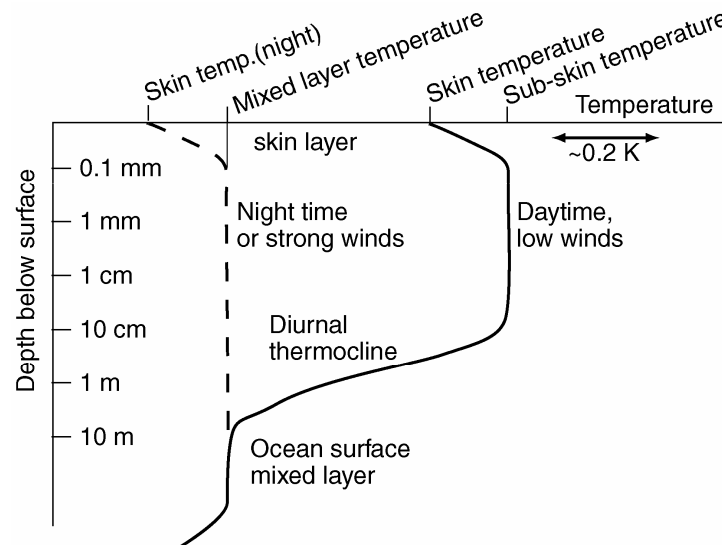


Figure 2-1: Schematic of the typical thermal structure near the surface of the ocean. The dashed line corresponds to conditions at night-time or of low insolation and strong winds. The solid line represents conditions of strong solar heating and low winds.

The need for in situ observations of skin SST is illustrated schematically by Figure 2-1 which shows the typical structure of temperature in the top few metres of the sea. Two factors cause the skin temperature of the ocean to differ from measurements sampled by more conventional thermometers on buoys or ships, which normally measure at a depth of between 1 and 8 m. Firstly under all conditions the surface microlayer, the upper 10 - 20 μm of water which determines the temperature detected by an infrared radiometer, is cooler by approximately 0.15 - 0.2 K compared to the sub-skin temperatures within 1 cm of the surface. Heat normally flows from the skin layer of the sea to the air even under strong sunshine since the solar flux penetrates deeper than this layer and delivers heat to the sea below the surface. The suppression of turbulence in the top few mm hinders heat reaching the surface from below, and hence the top microlayer cools slightly. Secondly solar heating tends to raise the temperature of the upper few metres during the day and, if the wind is too weak to mix this heat deeper, a diurnal thermocline develops. In this case the water temperature at 1 cm depth may be up to 1 or 2 K warmer than that measured at 5 or 10 m. Unlike the skin temperature deviation, which seems to be fairly predictable to within 0.1 K, the diurnal thermocline can vary rapidly over hundreds of metres horizontally and within tens of minutes, depending on the wind and cloud variability.

Both these effects, and particularly the latter, introduce considerable uncertainty when relating the skin temperature as measured by an infrared radiometer on a satellite to the *in situ* temperature measured by sensors on a buoy or the hull of a ship. This is unsatisfactory if the *in situ* measurements are used to validate satellite skin SST products. In that case they are not comparing like with like and such validations must be considered spurious unless there is a strong reason to expect that there is no diurnal thermocline present, as at night or under very strong winds. The most insidious problem is that under moderate winds there may still be a warming of a few tenths of a Kelvin that is not obvious but is nonetheless unacceptable when *in situ* data for validation are required to estimate the skin temperature to an accuracy of 0.1 K, in order that the AATSR SST product specification of better than ± 0.3 K can be tested.

For this reason *in situ* data for validating satellite-derived SST data products, which correspond to the skin temperature, must themselves be radiometric measurements of the skin temperature if they are not to introduce spurious errors into the comparison between the two. Hitherto very few such skin SST data have been routinely acquired by oceanographers. A programme of continuous high quality skin temperature monitoring using the M-AERI instrument run by RSMAS, Miami, has made data available for AATSR validation, but these measurements have now ceased. The cost of continuously manning the sensor to protect it from rain and spray made it prohibitively expensive to operate. To meet the need for continuous long-term monitoring of skin SST in temperate latitudes, at a reasonable cost, it became evident some years ago that ship-borne radiometers were needed that could be deployed autonomously on ships of opportunity. In this way they would be acquiring data at sea most of the time and thus able to add to the AATSR match-up database whenever the satellite passed over the ship in cloud-free conditions. This is what motivated the design and construction of the two ISAR instruments provided for the work described in this report.

2.2 The ISAR instrument

Ship-borne radiometry for measuring the skin SST is a very recent technology. The radiometric measurement of temperature to within ± 0.1 K is just as challenging at sea level as it is from space. Because the internally calibrated optical components of a radiometer must be identical to those in the target-viewing optical path, it is not possible to protect the fore-optics behind a protective front window. The marine environment is much less benign than that in space, and shipborne radiometers must be designed with great care if they are to maintain their calibrated accuracy for several weeks at a time in all weathers, including rain and salt spray. In order to protect the critical optical elements such as mirrors and blackbody surfaces they must be provided with a weather-proof shutter that closes as soon as any precipitation is detected.

Nonetheless some degradation is inevitable, and the sampling methodology allows for this by continuously referencing to two blackbody cavities of known temperature (one heated above ambient) and regularly replacing the radiometer every two to three months for calibration, maintenance and (when necessary) refurbishment of degraded optical parts. Thus continuous

operation throughout the year requires the use of two instruments that can be interchanged with each other.

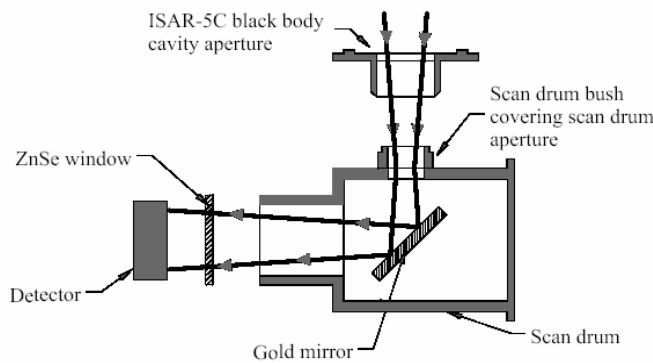


Figure 2-2; The fore-optics components of the ISAR, consisting of a ZnSe window through the weatherproof housing and the scan mirror inside its drum housing, shown here pointing into one of ISAR's blackbodies.

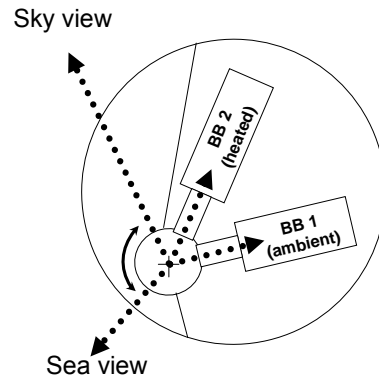


Figure 2-3; Section through ISAR and the scan drum, showing the arrangement for viewing the blackbodies, the sea and the sky.

The ISAR instrument consists of several subsystems described in outline as follows. The **fore-optics system** which routes the optical path from different targets to the detector is shown in Figure 2-2. The scan mirror is a gold 3 mm glass substrate front-surface mirror housed in a rotating protective scan drum driven by a computer controlled shaft encoder. Figure 2-3 shows how the scan mirror points the field of view successively at the different targets (sea, sky and both blackbodies), viewed via a small aperture cut into the scan drum wall that is the only place that water may enter into the instrument. The optical path includes a plane ZnSe window set deep within the ISAR instrument that completely seals the detector and the instrument electronics from the external environment. It is coated for a high infrared transmission of >90%. The scan drum is designed so that when the radiometer view field points outwards the blackbody cavities are closed, and when it points towards one of the blackbodies, the scan drum seals the blackbodies from ingress of water or salt spray.

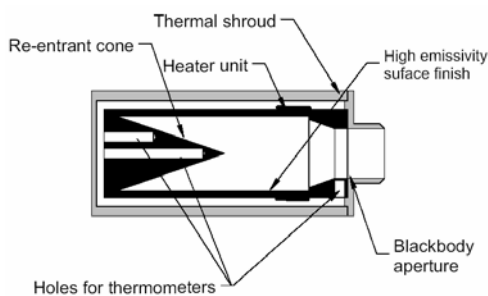


Figure 2-4; Section through one of the ISAR blackbody cavities



Figure 2-5; External view of the ISAR showing the shutter open. The optical rain sensor is in front

The **detector and blackbody calibration system** consists of a Heitronics model KT15.85D which delivers an analogue output dependent on incident radiation within a spectral band-pass of 9.6 -

11.5 μm over a temperature range of 173 - 373 K. During an operating cycle it views sea, sky and two calibration blackbodies housed within the ISAR. The blackbodies (see Figure 2-4) were designed with a re-entrant cone base and a partially closed aperture to have an infrared emissivity greater than 0.999. Three precision thermistors (having a NIST traceable calibration to ± 0.05 K) are used to monitor the temperature of each blackbody.

The **environmental protection subsystem** incorporates a storm shutter and an optical rain detector. Whenever the rain detector output rises above a threshold indicating precipitation (or dust particles) the scan drum immediately points inside the ISAR to protect the fore-optics and an external shutter rotates circumferentially to cover the 150° viewing port (shown open in Figure 2-5). When the rain detector output falls below the threshold for a sufficient period (normally 10 min) the shutter re-opens and monitoring resumes.

The **internal control and data acquisition system** is an on-board computer chip that manages the viewing cycle, controls the shutter operation, performs the analogue-to-digital conversions for the radiometer and thermistor outputs and logs the data. It also monitors a number of other variables logged in the ISAR, such as GPS location and time which uniquely identify every data record, pitch and roll, power supply voltages and the ambient temperature inside the ISAR. It operates the measurement cycle which, for this validation work, is set at 40 samples viewing the sea, 30 samples each viewing the two blackbodies and 10 samples viewing the sky, a cycle which takes about 140 s to complete. It uses the blackbody views to calibrate the detector and then uses the sea and sky views to calculate the skin temperature of the sea, making allowance for sky reflection and the non-blackness of the emission from the sea. It logs the average values for each scan cycle on internal flash memory and sends the full resolution data to an external logging computer. However, it is capable of autonomous operation independently of the external computer.

The **external interface** uses RS232 protocol to communicate with the external logging computer. The interface also allows for ancillary atmospheric and ocean monitoring sensors mounted on the vessel to be powered and to submit their data into the ISAR's internal data logging system.

The subsystem components described above are housed in a compact (570 x 220 mm) cylinder shown in Figure 2-5. Figure 2-6 shows the ISAR in its operating position, viewing the sea surface at an incidence angle of 25° when mounted on the bridge wing of the P&O vessel *Pride of Bilbao*.



Figure 2-6: The ISAR and rain detector mounted on the *Pride of Bilbao*.

2.3 Operational deployment of ISAR

The ISAR is installed on the P&O Ferry *Pride of Bilbao*, which sails regularly from Portsmouth to Bilbao and back, crossing the English Channel and the Bay of Biscay. The ISAR instrument is mounted on the top of the starboard Bridge Deck, as shown in Figure 2-7 and Figure 2-8. The *Pride of Bilbao* is scheduled to be at sea most of the time with only brief turnarounds in port, thus maximising the opportunities for match-ups with AATSR, except when the vessel is laid up for refit and maintenance for a few weeks in winter.



Figure 2-7; The P&O Vessel, *Pride of Bilbao* viewed from the port side. The arrow marks the location, on the starboard side, where the ISAR is installed.



Figure 2-8: A view from below the ISAR on the *Pride of Bilbao* bridge.

There is no need for an operator to travel with the vessel. The ISAR is set running prior to a deployment and then operates autonomously. It is connected by the RS232 interface to an external computer located in the radio room of the *Pride of Bilbao*. ISAR can be manually controlled through this interface, but its continued autonomous operation is independent of the status of the external computer. The logging computer receives the full resolution data stream from the ISAR and estimates SST based on the raw counts from the detector.

In addition the computer records the following ancillary data, each with a date and time stamp from the same source:

- Wind speed and direction relative to the ship
- Roll and pitch
- GPS position, GPS time and ship velocity derived from GPS
- SST measurements by hull mounted thermometers
- Atmospheric humidity
- Long-wave downward radiation
- Total downward radiation
- Solar azimuth and zenith angle

Throughout Phase 2 of the project a subset of the logged data was packaged and transmitted in near-real time (every four hours) by Iridium satellite to the project base at NOCS. This allows immediate monitoring of the ISAR performance through analysis of the gain factor set by the internal blackbody views. If this is satisfactory the *provisional* SST data are made available through the project web page (www.isar.org.uk) in near-real time.

Should the gain factor go outside expected limits, implying undue degradation of optical components, the installation is inspected at its next visit to Portsmouth docks, normally within the next three days. If minor in situ maintenance does not solve the problem the instrument is exchanged with the spare and removed for full maintenance in the laboratory at NOCS.

2.4 Calibration and validation of the ISAR instrument

As described more fully in the Final Report following Phase 1, the accuracy of the SST measurements made by ISAR is achieved, and their quality is assured, by a three stage procedure:

1. The raw counts from the sea and sky view are converted into equivalent brightness temperatures using the views of the two blackbodies internal to the instrument during the same measurement cycle, along with the associated thermistor temperatures. This internal calibration procedure automatically allows for any gradual degradation of the optical pathway.
2. An external calibration / validation procedure is performed on the ISAR instrument in the laboratory before and after every deployment. This involves the viewing of a specially-designed high quality blackbody over a period of several hours while its temperature is slowly raised. Comparison between the ISAR-derived temperature and the blackbody temperature as measured by a platinum resistance thermometer provides a validation of the ISAR's internal calibration process. If necessary, it allows fine adjustments to be made to the coefficients used in the SST retrieval calibration algorithm. The ISAR is not deployed unless this laboratory calibration shows agreement between the ISAR and the external blackbody temperatures that is better than 0.1 K. Similarly, if the post-deployment laboratory calibration does not show the same agreement, the data acquired during that deployment are not used for AATSR validation purposes unless a thorough analysis can identify and eliminate the source of the discrepancy.
3. The laboratory blackbody is the CASOTS-2 instrument (see Figure 2-9) built specially for the project and described in the Phase 1 Final Report. Its performance is compared periodically against a reference blackbody which is traceable to an internationally accepted standard.

During Phase 2 of the project, a small but significant revision was made to the algorithm used for converting raw counts to brightness temperature within Stage 1. Essentially this replaces a fixed estimate of an effective emissivity for the internal blackbodies by a value which can change slightly as a function of the internal gain measured by viewing the two internal blackbodies. The details of the change are elaborated in Appendix A. A tuneable constant is required for this new algorithm but, having derived it in the first instance by matching the results to the post-deployment calibration of a single dataset, it turns out that the same constant is applicable to all the deployments, giving confidence that the constant is a function of the internal optical architecture of the instrument and largely independent of the degree of optical degradation.

Since introducing this improvement to the SST retrieval algorithm, the lab calibrations before and after deployment appear to be almost identical. Although we still perform a post-deployment reprocessing of the SST retrievals before using the data for AATSR validation, the differences between the final validated SST product and the near-real time provisional SST product retrieved via Iridium are now very small.

In March 2006, the CASOTS-2 laboratory blackbody system was taken to RSMAS, Miami, Florida, USA, for intercomparison tests with the M-AERI instrument. Both a M-AERI and an ISAR served to provide a cross calibration between the CASOTS-2 and a reference blackbody used by RSMAS which has a calibration traceable to NIST standards. The intercomparison tests were successful, demonstrating that the CASOTS-2 reference blackbody performance is comparable with the reference blackbody used in USA. Appendix C gives further details of the tests.

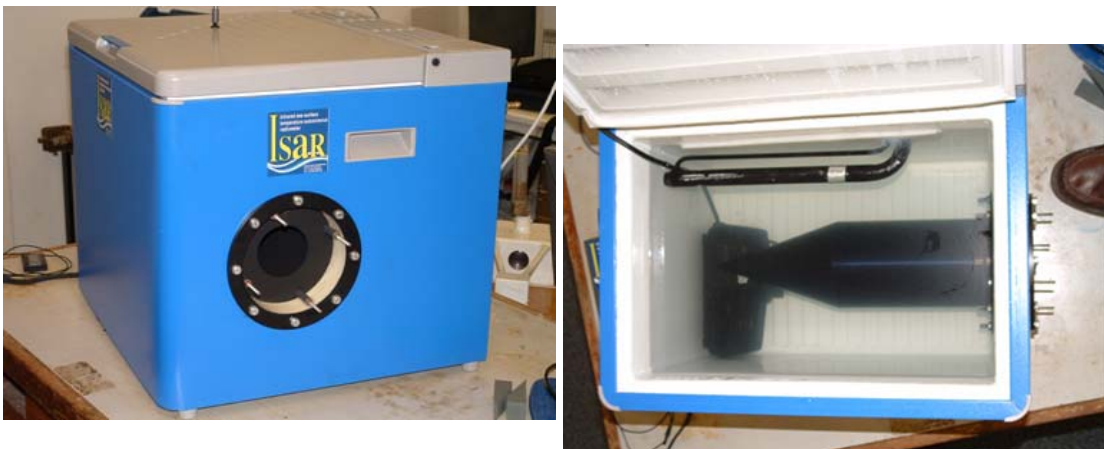


Figure 2-9: The CASOTS-2 blackbody used as the laboratory reference for calibrating or validating the ISAR before and after each ship deployment. **Left:** External view showing the blackbody cavity aperture and blanking plates. **Right:** Internal view of the water bath revealing the conical end of the cavity. The black object to the left is the pump for stirring.

2.5 ISAR Performance

ISAR was the first infrared ship-borne radiometer to demonstrate that it can operate truly autonomously. During Phase 2 it has continued to prove its capability for unattended operation for up to three months between servicing. We have continued to learn from experience and to make minor refinements to its design, but problems have been even fewer during Phase 2 than they were during Phase 1. Although mirror degradation is inevitable, it has been reduced since a new mirror type was sourced. Even more important is that the use of the new SST retrieval algorithm mentioned in section 2.4 has proved capable of keeping the SST measurement accuracy well within the specification of ± 0.1 K right through to the end of each deployment. Only one major failure of ISAR was experienced during Phase 2 when the main scan drum seized up, fortunately shortly before a planned instrument exchange. The likelihood of a recurrence has been reduced by subsequently paying closer attention to the alignment and shaft adjustment during maintenance. A

summary of the minor modifications made to the instruments during Phase 2 are provided in the Instruments' service logs in Appendix E.

The successful deployments during Phase 2 have reinforced the conviction gained during Phase 1 that the ISAR system for radiometrically measuring sea surface skin temperature from ships of opportunity provides a reliable and effective means of acquiring data for validating satellite-derived SST data products. Following publication of the scientific paper describing the instrument there has been an expression of interest from other groups around the world in using similar radiometers.

3. Measurements made by the ISAR System

This chapter reports the measurements that have been obtained during Phase 2 of the contract. The first part identifies all the data that were collected using the ISAR system on *Pride of Bilbao*. The second reports the information about skin SST that can be drawn from the ISAR measurements. The third part confirms the number of match-ups that were obtained between *in situ* skin temperature measurements from ISAR and coincident clear-sky SST retrievals from AATSR.

3.1 Data collected from ISAR deployments

Figure 3-1 shows the timing of each deployment since the start of the contract on March 1st 2004. Phase 2 commenced on March 1st 2006 and comprises deployments D10 to D18. It can be seen that one of the two ISARs (labelled ISAR-002 and ISAR-003) was at sea for almost all the time, apart from the annual refit of the *Pride of Bilbao* in January each year.

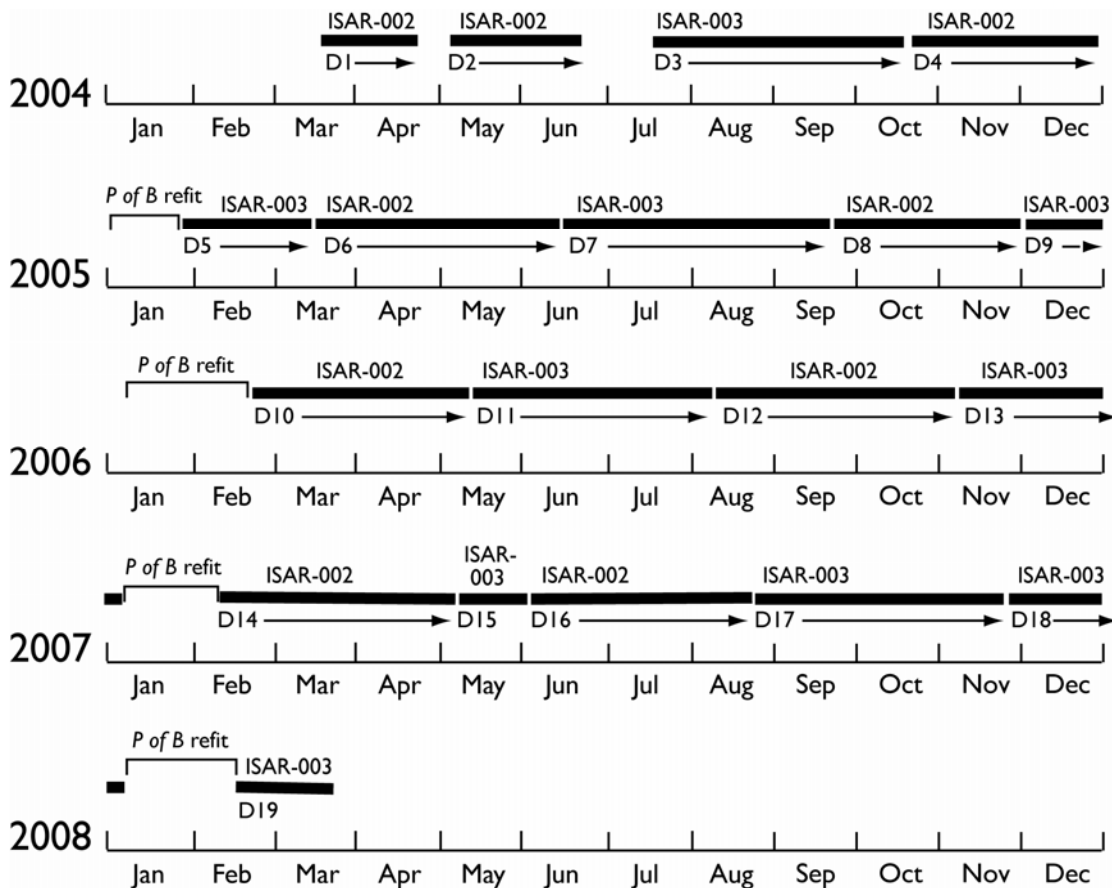


Figure 3-1: Time-line for Phase 1 and Phase 2 showing when the ISAR system was operating on *Pride of Bilbao* during March 2004 to February 2008, which of the two instruments was deployed, and the deployment reference (D1 etc.) assigned to each deployment.

Throughout Phase 2 of the project the ship operated a three-day cycle between Portsmouth and Bilbao, with a similar cruise track to that shown in Figure 3-2. A summary of the different

deployments, defining their start and end dates, the ISAR instrument used, a list of the ancillary data available, brief notes of the quality of skin data acquired and the number of validation match-ups provided to the AATSR Validation Scientist is provided in

Table 3-1.

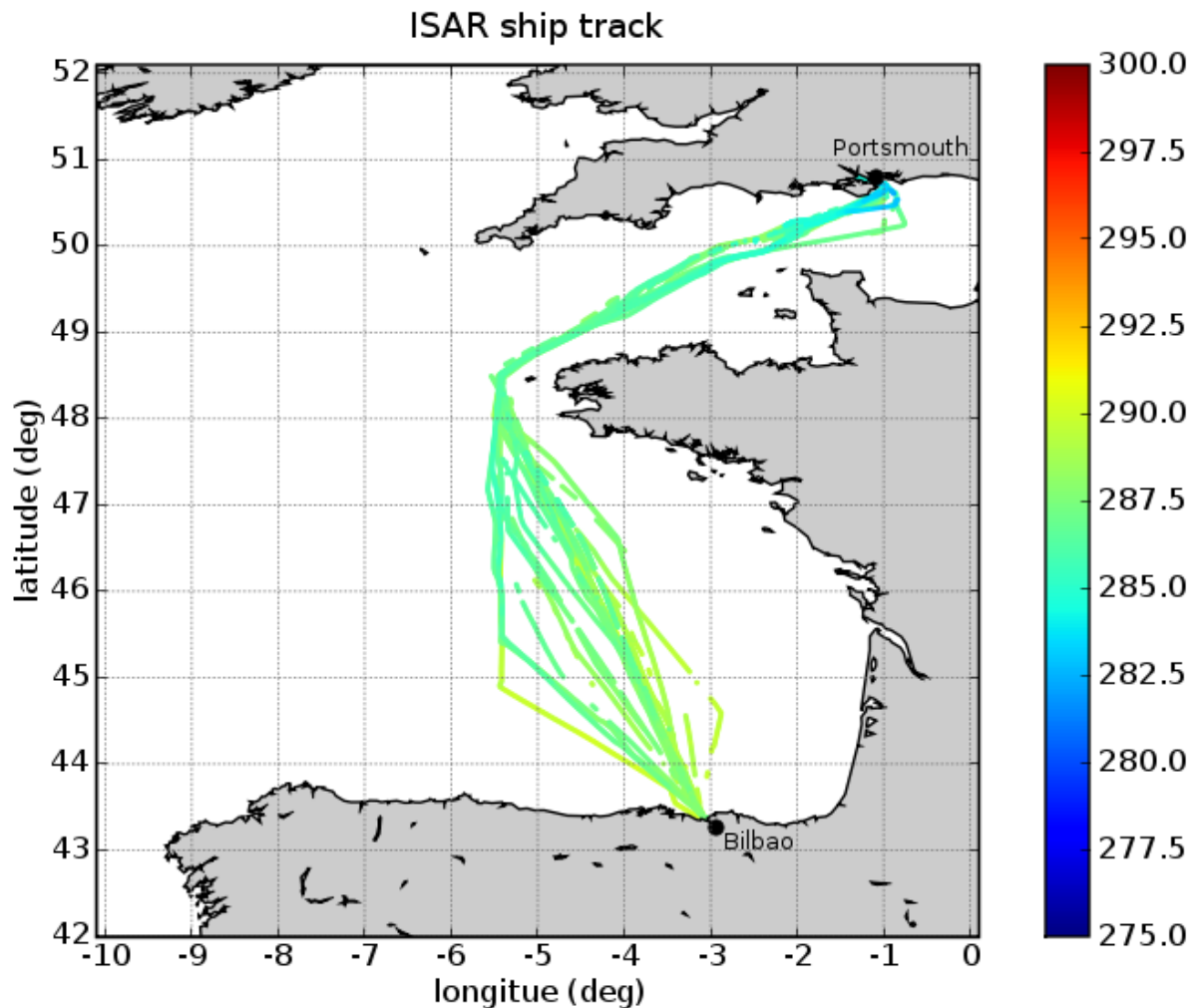


Figure 3-2: Ship track of the *Pride of Bilbao* during the period 6 Nov 2006 to 4 Jan 2007. (deployment D13). Each skin SST temperature measurement obtained by the ISAR is plotted as a dot, colour coded according to the scale beside the figure, which is in K. In this late autumn period the temperature is between about 10°C and 16°C.

The full suite of sensors (see list in section 2.3) was installed on the *Pride of Bilbao* throughout Phase 2 of the project, with occasional removals for service or calibration. A full list of all the individual data files acquired for each deployment is given in Appendix B. These are held in the project database at NOCS and securely backed up in archive storage. Access to the full database of raw data files can be arranged by contacting W. Wimmer at NOCS. There is a provisional skin SST estimate available before the deployment has ended, which can be accessed by registered users via <http://www.isar.org>. When the post-processing has been performed, the final skin temperature products can be obtained from the ISAR web page by registered users.

Table 3-1: Primary information about each deployment during Phase 2.

No.	Dates	ISAR	Ancillary data	Notes	Match-ups achieved ³
D10	21 February to 10 May 2006	002	PIR, PAR , Pyranometer, Anemometer , Dew pt. temp. * Hull temp * . Minipack * (* from 27 Feb)	Problem-free deployment. Scheduled completion	78
D11	10 May to 9 August 2006	003	PIR, PAR , Pyranometer, Anemometer , Dew pt. temp. Hull temp. Minipack Additional hull thermistors	Problem-free deployment. Scheduled completion	142
D12	9 August to 6 November 2006	002	PIR, PAR , Pyranometer, Anemometer , Dew pt. temp. Hull temp. Minipack Additional hull thermistors	Problem-free deployment. Scheduled completion. However, post-deployment inspection and calibration showed mirror failure, which could be traced by the gain diagnostics to have occurred on 26 October, invalidating data from the last 10 days of D12	121
D13	6 December 2006 to 4 January 2007	003	PIR, PAR , Pyranometer, Anemometer , Dew pt. temp. Hull temp. Minipack Additional hull thermistors	Problem-free deployment. Scheduled completion at start of vessel's annual refit. Final calibration good, but mirror showed signs of degradation and was replaced.	29
D14	8 February to 8 May 2007	002	PIR, PAR , Pyranometer, Anemometer * , Hull temp. Minipack Additional hull thermistors (* from 20 March)	Problem-free deployment. Scheduled completion. First deployment with new type of scan mirror confirmed that the LBP mirror is much better suited than the previous OFR mirror for use in the ISAR optical path.	206
D15	8 May to 1 June 2007	003	PIR, PAR , Pyranometer, Anemometer , Hull temp. Minipack Additional hull thermistors	Mechanical failure of scan drum. Deployment aborted. No data acquired.	0

³ This is the number of matches within 2 hrs and 1 km of an AATSR pixel, corresponding to the data delivered to the AATSR Validation Scientist.

No.	Dates	ISAR	Ancillary data	Notes	Match-ups achieved ³
D16	4 June to 24 August, 2007	002	PIR, PAR , Pyranometer, Anemometer , Hull temp. Minipack Additional hull thermistors	Problem-free instrument operation. Scheduled completion of deployment, Discovered that failure of UPS had closed down logging computer on 7 August , but ISAR-002 continued to function and logged internally..	139
D17	24 August to 25 November 2007	003	PIR, PAR , Pyranometer, Anemometer , Hull temp. Minipack Additional hull thermistors	Problem-free instrument operation. Scheduled completion of deployment, Fault discovered in GPS aerial connection on 21 November prevented data logging for final 3 days of deployment	275
D18	29 November 2007 to 7 January 2008	003	PIR, PAR , Pyranometer, Anemometer , Hull temp. Minipack Additional hull thermistors	Problem-free instrument operation. Scheduled completion of deployment at start of vessel refit.	11

3.2 The variability of skin SST in the Bay of Biscay

The temperatures measured by the ISAR when not closed for protection from precipitation and spray make up an impressive set of measurements defining the variability of the skin temperature of the Bay of Biscay and English Channel over nearly two years.

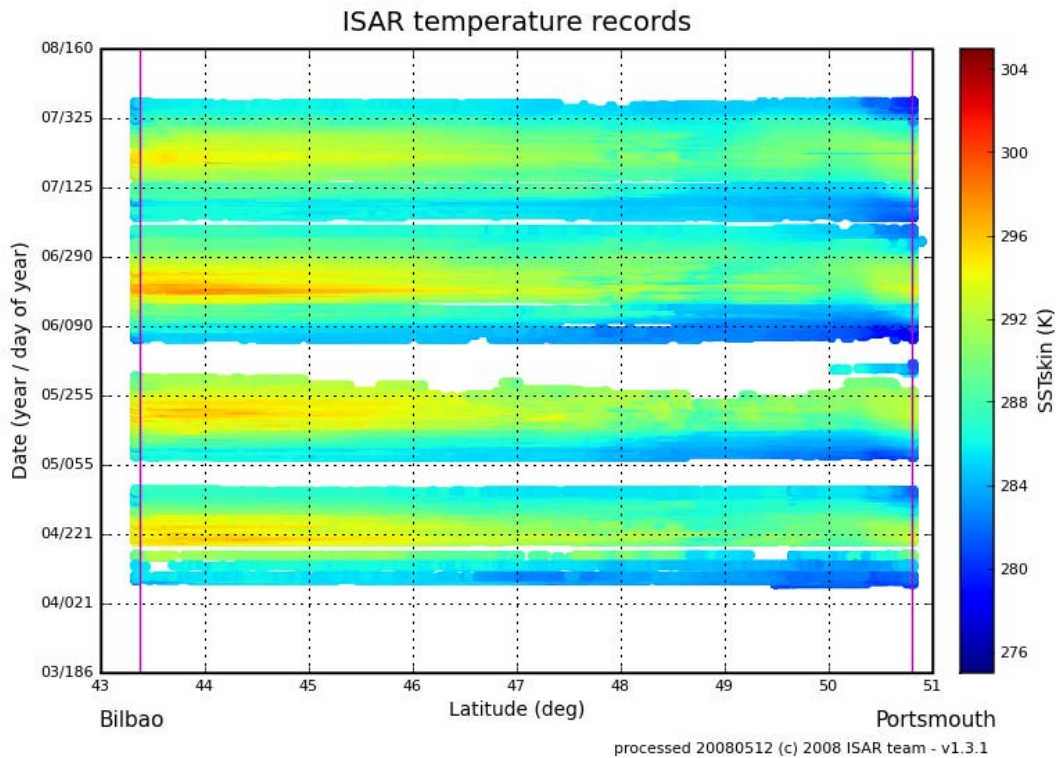


Figure 3-3 shows a latitude-time plot of the complete four-year ISAR skin temperature record. This shows the position (in latitude) along the cruise track in the x axis and the date-time in the y axis. The colours represent the skin temperature. As expected the SST record is warmer towards the left of the figure which is the Bilbao end of the ferry's route, and cooler to the right (the Portsmouth end). Over the four years the figure shows that the ISAR encountered temperatures as low as about 5°C and as high as about 25°C. The seasonal pattern is evident in the figure, while it appears that ISAR sampled the highest temperatures in 2006.

The gaps on the figure show when no data were acquired. The regular January refit causes an annually occurring gap. The figure also shows that in general the two years of Phase 2 (the upper half of the figure) had fewer missed sampling opportunities than Phase 1 because of instrument failure or overcautiously set precipitation thresholds for closing the weather shutter.

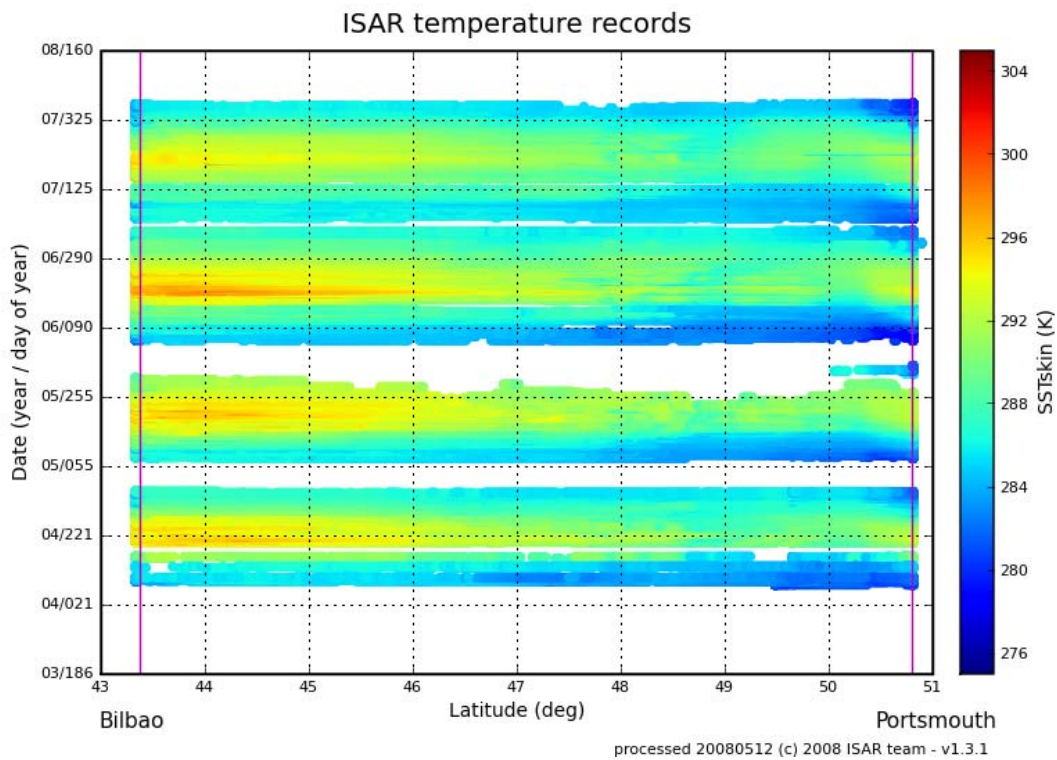


Figure 3-3: Latitude-time plot of the full project record of skin SST from March 2004 to January 2008. The temperature in °C can be derived from the temperature as shown in K by subtracting 273.15

Figure 3-4 shows the geographical location of all the tracks when the ISAR was sampling. Because the lines overprint each other in the plot, the colours shown come from the most recent tracks. The value of this plot is in showing how the ship deviates quite widely from its basic path, especially in the Bay of Biscay where it is less constrained by traffic management rules. This is useful for the purposes of validation since it broadens the variety of SST structures encountered.

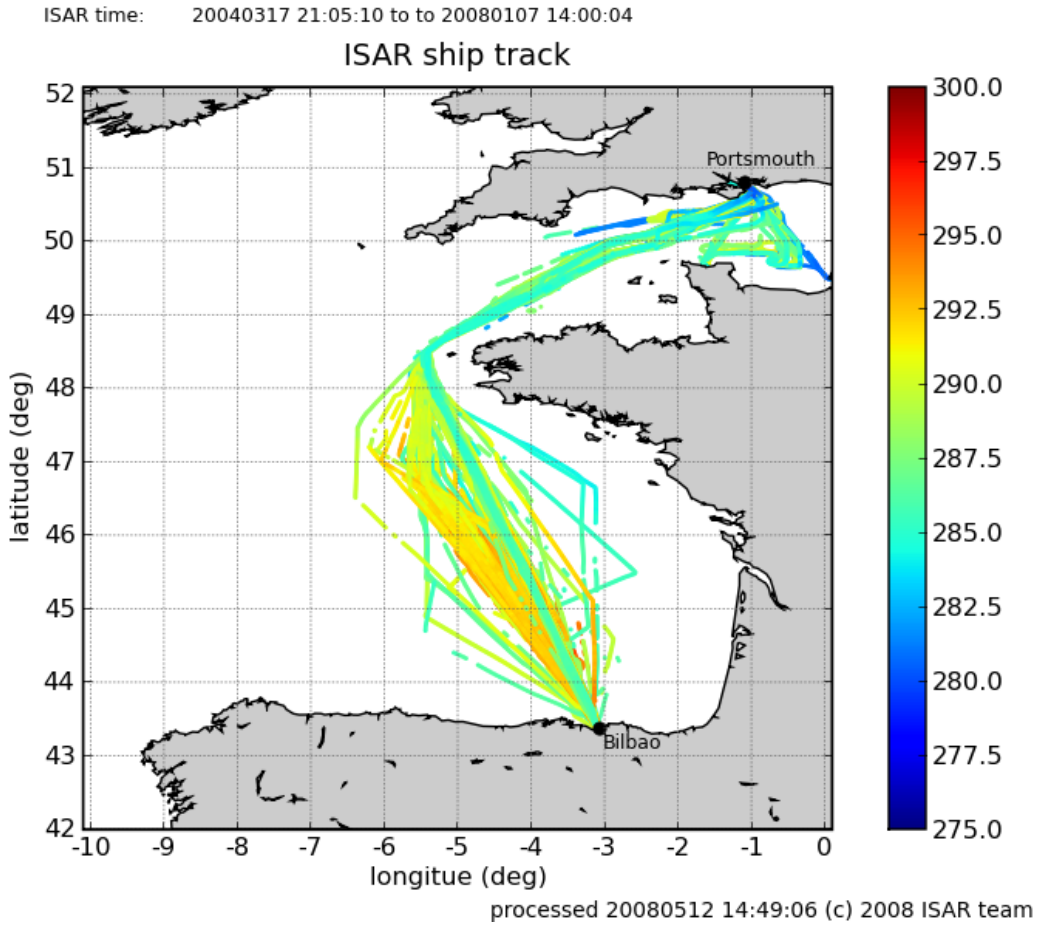


Figure 3-4: Cumulative picture of all sample tracks, coloured according to temperature, when data were acquired by ISAR over the full four years of Phase 1 and Phase 2.

3.3 Match-ups between ISAR and AATSR samples

3.3.1 Basis for defining coincidence between ISAR records and AATSR pixels

Having secured the operational supply of *in situ* skin SST along the *Pride of Bilbao* cruise track, these data are then matched to any coincident AATSR observations. The question here concerns how much flexibility is allowed in the definition of “coincidence” in space and time between ship and satellite samples.

The size of the match-up dataset depends on how stringent is the definition of data coincidence. If the requirement is too severe then there will be very few matches. If it is not severe enough then a large number of the matched pairs will be from quite different parts of the sea. Until we had the experience from which to identify the optimum matching criteria, we adopted an approach which specified five different grades of severity. These relate to the search radius, $N\Delta x$, for spatial coincidence and the time window, $M\Delta t$, for temporal matching, as illustrated in Figure 3-5.

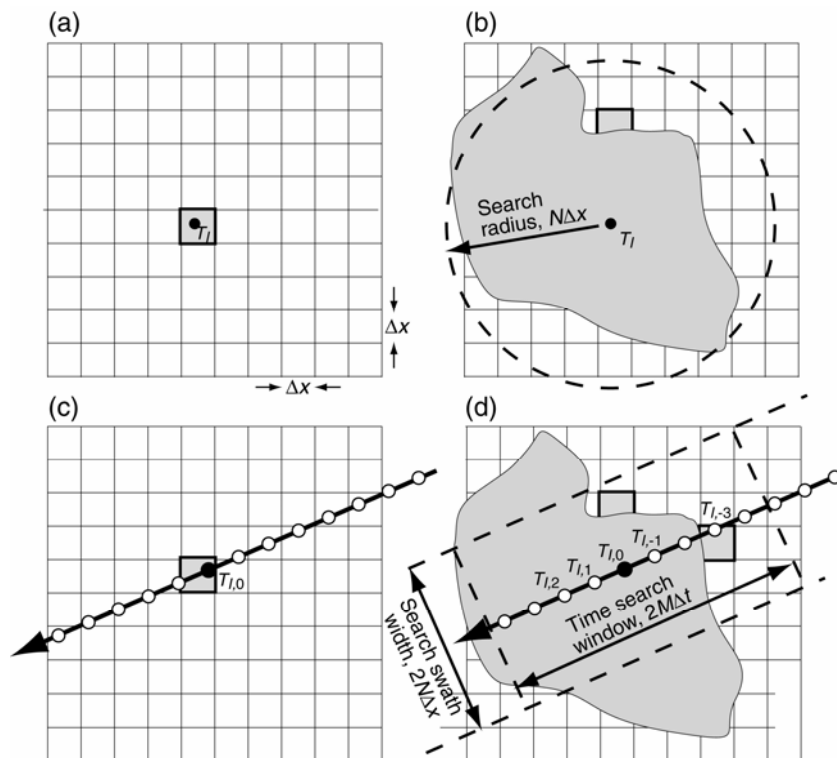


Figure 3-5: Examples of match-up situations encountered in the construction of a match-up database. (a) Point sample when there is no cloud. Match the *in situ* sample closest to the time of the overpass to the pixel in which it lies. (b) Point sample obscured by cloud. Match the *in situ* sample closest to the time of the overpass to the closest cloud-free pixel. The search radius needs to be limited to N pixels. (c) Along-track sensor such as ISAR in cloud free conditions. Match the *in situ* sample closest to the time of the overpass to the pixel in which it lies. (d) Along-track sensor in cloudy conditions.

We have matched the ISAR record to the corresponding AATSR image datasets according to a set of criteria graded as follows for severity:

<u>Grade</u>	<u>Match-up Criteria</u>
1	Coincidence of ISAR and AATSR sample within ± 2000 s time window and 1 km search radius in space.
2A	Temporal match within ± 2000 s and spatial match within ± 20 km
2B	Temporal match within ± 2 hrs and spatial match within ± 1 km
3	Temporal match within ± 2 hrs and spatial match within ± 20 km.
4	Temporal match within ± 6 hrs and spatial match within ± 25 km

Grade 1 corresponds to the closest coincidence considered feasible, within 1 km spatially and about half an hour in time, and effectively yields a match to the pixel containing the ship at the time of the overpass.

Grade 2A allows a match to the nearest cloud free pixel to the ship track within a radius of 20 km.

Grade 2B limits the search radius to 1 km but allows a match to an earlier or later part of the ship track within a time window of 2 hours either side. **This is the matching criteria adopted by the AATSR Validation Protocol and thus it provides the core set of validation data.**

Grade 3 allows matches with both the wider spatial search radius and the extended time window. This corresponds to the widest flexibility that we considered, at the start of the project, to be feasible in the English Channel / Bay of Biscay region.

Grade 4 represents the coarsest of the criteria used by many agencies for open ocean validation of satellite SST data. It was not used in Phase 1 but has been added since it is one of the cases specified by the GODAE high-resolution sea surface temperature pilot project (GHRSSST-PP).

This approach often leads to multiple matches for a given overpass. When this occurs the AATSR-ISAR matches are treated as independent as long as neither the same AATSR pixel nor the same ISAR sample are used for a different matched pair. If this should occur the closest in distance is selected. The matching algorithm rejects any matches found at locations corresponding to the ship being in port, or close to port, where it is unlikely that the ISAR and AATSR are properly viewing the sea surface temperature.

As far as possible, we have sought to produce a processing system which operates automatically without human intervention. Thus given a file or files containing the calibrated record of an ISAR deployment, and access to the AATSR data files covering the same period of time as the deployment, the program must find the matched pairs for different grades of coincidence criteria, and then evaluate the mean and standard deviation of the differences for all matched pairs corresponding to a particular grade. There are two good reasons for using an automatic system. The first is that, once the system has been developed and validated, it significantly reduces the effort

involved, leads to much more rapid matching of ISAR to AATSR data, and thus facilitates near-real time monitoring of AATSR performance as long as the ISAR data can be transmitted to base soon after acquisition. Secondly it avoids the need for subjective decisions to accept or reject match-ups, which might bias the matching and thus the validation process. It should be noted that, having identified the matches available for analysis, the program excludes from the bias evaluation any points lying outside three standard deviations of the set of observations being analysed.

During Phase 2 a study was performed to provide a more objective estimate of the quality of a given match-up pair of data in relation to a variety of factors that affect whether we are truly comparing like with like. This study has resulted in the formulation of a completely different set of quality indicators for each match-up pair, ranging in value from 0 to 3 where 0 is the poorest and 3 is the best quality. This is explained below in section 5.1 and elaborated in the separate report on Work Package 700. Note that the order of expected goodness of match for the Quality Value, Q, (higher number = higher quality of match) is the reverse of that for the Grades (grade 1 = best match). This was done to make the new match-up quality indicator consistent with other quality flags applied to SST datasets.

3.3.2 Numbers of matches achieved between ISAR and AATSR

Here we report the numbers of matches that have been achieved during the project so far in both Phase 1 and Phase 2. Since the reprocessing of the raw ISAR data, the number of matches from Phase 1 has changed slightly which is why both are reported here. Discussion of how the ISAR temperatures compare with the AATSR SST products is left to section 4. Our concern is first to demonstrate that the use of the ISAR, deployed autonomously on a ship of opportunity that spends most of the time at sea on a regular route, has delivered many more validation opportunities than were previously available from occasional dedicated validation campaigns.

The number of validation match-ups varies not only with the grade of coincidence, but also with the type of AATSR data product being considered. There are four AATSR SST data products generated by different algorithms, labelled as follows:

- | | |
|----|---|
| D2 | The dual view 2-band algorithm using the 11 and 12 μm channels from both the nadir and forward views. |
| D3 | The dual view 3-band algorithm using the 3.7, 11 and 12 μm channels from both the nadir and forward views. |
| N2 | The nadir-only 2-band algorithm using the 11 and 12 μm channels from only the nadir view. |
| N3 | The nadir-only 3-band algorithm using the 3.7, 11 and 12 μm channels from only the nadir view. |

Table 3-2 summarises the number of matches achieved during the whole project. It is broken down by AATSR algorithm type, and the results are presented for each grade of severity of space-time coincidence.

The 3-band algorithm can be used only at night when there is no problem of solar reflection in the 3.7 μm waveband. The 2-band algorithm can be used both day and night, but since the standard AATSR products normally provide only 3-band products at night, we have only counted the number of 2-band products from day overpasses. Note that there tend to be more matches with data produced by the nadir-only algorithms because in patchy cloud the forward views are more frequently flagged as cloudy than the nadir view, hence there are more nadir-only SST pixels than dual-view.

Table 3-2: Total numbers of match-ups during the whole project, between ISAR and AATSR skin SST measurements, for different satellite products and different grades of match-up coincidence.

AATSR product type	Grade 1	Grade 2a	Grade 2b (AATSR Validation Protocol)	Grade 3	Grade 4
D3 (night)	281	392	972	1411	4548
D2 (day)	157	249	677	941	2742
N3 (night)	453	815	1549	2883	9802
N2 (day)	336	768	1339	2745	8171

4. Validation of AATSR against ISAR data

In this section, the differences between the AATSR SST retrievals and coincident ISAR data are summarised across the whole four year dataset from March 2004 to February 2008. Here the data have been amalgamated into a large database. Detailed information about the matches from individual deployments can be found in the quarterly reports submitted to Defra, and tables summarising the match-up statistics for individual deployments are shown in this section. These tables and associated graphs test for any trends in the product accuracy.

It has not been possible to fully amalgamate all the data into a single dataset because changes were made to the AATSR algorithm coefficients, operational from December 7th 2005⁴. At the time of writing, ESA were still reprocessing the AATSR data before December 7th 2005, using the new coefficients, so we have not yet been able to acquire any data from before that change. Therefore it is not appropriate to attempt a single validation across the whole period. Instead we apply the validation in two stages, before and after the algorithm change.

In the rest of this section we consider separately the validation of the dual view algorithms (section 4.1) and the nadir-only algorithms (section 4.2). Section 4-3 compares the dual view and nadir-only data and considers the validation of 2 channel data acquired at night.

4.1 Dual view algorithms

The primary SST product of the AATSR is that retrieved from the dual view. The comparison between the SSTs retrieved from the AATSR dual view two-waveband (D2) and three-waveband (D3) algorithms and the coincident ISAR measurements is shown in Table 4-1 and Table 4-2. These show extremely good agreement between the in situ and the satellite temperatures. The bias is less than 0.1 K for all grades of match-up for both the D2 and D3 products, which means it is effectively indistinguishable from zero at the level of accuracy to which the ISAR itself is validated.

Comparing the biases before and after the algorithm change shows very little difference. For the two-waveband algorithm the slight negative bias shifts to a slight positive bias after the algorithm change, but for the three waveband algorithm there is no change detectable above the 0.1 K specification limit of the ISAR. This is evident when comparison is made with Table 4-3, which contains the amalgamated match-ups statistics for the whole of Phase 1 and 2.

⁴ A new set of SST retrieval coefficients came into operation within the AATSR processing chain on 07 December 2005. The retrieval coefficients previously in use were based on the same atmospheric spectroscopy as was used for ATSR-1 and ATSR-2, which pre-dated the more recent releases of the HITRAN molecular spectroscopy database. This new set of retrieval coefficients are based on the HITRAN 2000 database.

The standard deviation about this very low mean bias is also small, although more variable with the match-up grade. For the Grade 2b match-ups that are used in the AATSR validation programme, the values are around 0.30 K for D3 and 0.44 K for D2. Given the natural variability in the ocean and the difficulty of ensuring that the *in situ* and the satellite sensors are precisely observing the same place, these are low standard deviations, which provide confidence in the atmospheric correction of the AATSR data. However, it will be show in Section 5.1 that these can be reduced further by taking account of the factors that introduce spurious mismatch errors that have nothing to do with the performance of either the AATSR or the ISAR.

Table 4-1: Statistics for match-ups (AATSR dual-view SST - ISAR) for Phase 1 before 7th December 2005, showing the bias and standard deviation, the number of matches, the number of overpasses from which they came, and the range of sea temperatures spanned by the match-up database.

Grade of coincidence	Mean bias, AATSR - ISAR	Standard deviation	No. of Matches	Overpass numbers	Min temp, °C	Max temp, °C
2 waveband algorithm (D2)						
1	-0.11	0.38	78	13	7.5	19.2
2a	-0.02	0.54	88	24	7.5	19.7
2b	-0.07	0.47	327	30	7.5	25.6
3	-0.06	0.55	385	42	7.5	25.6
4	-0.19	0.61	1154	56	7.5	25.6
3 waveband algorithm (D3)						
1	0.10	0.29	68	8	11.9	20.4
2a	-0.04	0.44	112	16	8.2	21.3
2b	0.05	0.32	232	16	7.8	20.9
3	0.00	0.37	425	27	7.3	21.6
4	-0.07	0.47	1428	58	7.3	22.5

Table 4-2: Statistics for match-ups (AATSR dual-view SST - ISAR) for Phase 1 after 7th December 2005 and Phase 2, showing the bias and standard deviation, the number of matches, the number of overpasses from which they came, and the range of sea temperatures spanned by the match-up database.

Grade of coincidence	Mean bias, AATSR - ISAR	Standard deviation	No. of Matches	Overpass numbers	Min temp, °C	Max temp, °C
2 waveband algorithm (D2)						
1	0.02	0.39	81	25	6.4	18.4
2a	0.10	0.95	164	43	6.4	20.4
2b	0.00	0.40	349	44	6.0	20.9
3	0.04	0.69	555	57	5.6	21.4
4	0.10	0.76	1588	103	5.6	24.1
3 waveband algorithm (D3)						
1	0.03	0.22	212	31	9.5	22.1
2a	0.02	0.33	280	44	8.7	22.1
2b	-0.03	0.30	741	43	9.2	22.6
3	-0.05	0.39	986	66	7.7	22.6
4	-0.08	0.48	3120	106	7.4	24.9

Table 4-3: Amalgamated table of match-ups (AATSR dual-view SST - ISAR) for all Phase 1 and Phase 2 showing the bias and standard deviation, the number of matches, the number of overpasses from which they came, and the range of sea temperatures spanned by the match-up database.

Grade of coincidence	Mean bias, AATSR - ISAR	Standard deviation	No. of Matches	Overpass numbers	Min temp, °C	Max temp, °C
2 waveband algorithm (D2)						
1	-0.04	0.36	157	38	6.4	19.2
2a	0.07	0.78	249	67	6.4	20.4
2b	-0.04	0.44	677	72	6.0	25.6
3	0.01	0.64	941	95	5.6	25.6
4	-0.03	0.71	2742	118	5.6	25.6
3 waveband algorithm (D3)						
1	0.04	0.25	281	38	9.5	22.1
2a	0.00	0.36	392	59	8.2	22.1
2b	-0.01	0.30	972	58	7.8	22.6
3	-0.03	0.39	1411	93	7.3	22.6
4	-0.08	0.47	4548	112	7.3	24.9

The validation locations for the Grade 2b match-ups are spread along the line of the ship track, as shown in Figure 4-1. Because of the ship's regular passenger timetable phase-locked to the daily cycle like the sun-synchronous orbit of Envisat, there is a tendency to sample day and night overpasses in different parts of the orbit, although there is a small overlap in places. There is no reason to expect that this should influence the bias measurements in any way. However, since the region off Ushant where the SST is spatially more variable is normally traversed during the day, this may account for the slightly higher variance from the 2-waveband match-ups.

The scatter plots of the dual view validation pairs, shown in Figure 4-2 and Figure 4-3 for before and after the 7th Dec 2005 algorithm change respectively, demonstrate graphically how good the matches are for both the 2-waveband and 3-waveband dual view retrievals, and the spread of temperatures over which they extend.

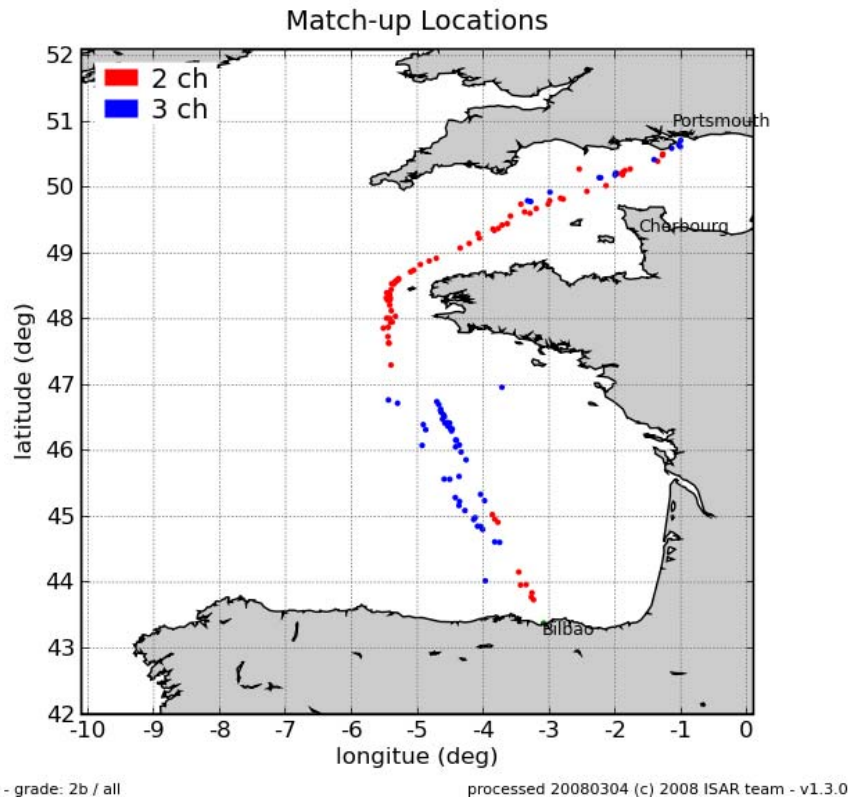


Figure 4-1: Location of the match-ups at Grade 2b coincidence for AATSR dual view SST retrievals against ISAR observations from four years of deployments on *Pride of Bilbao*, 2004-2008. The colours distinguish 2-waveband data (day: red) from 3-waveband data (night: blue).

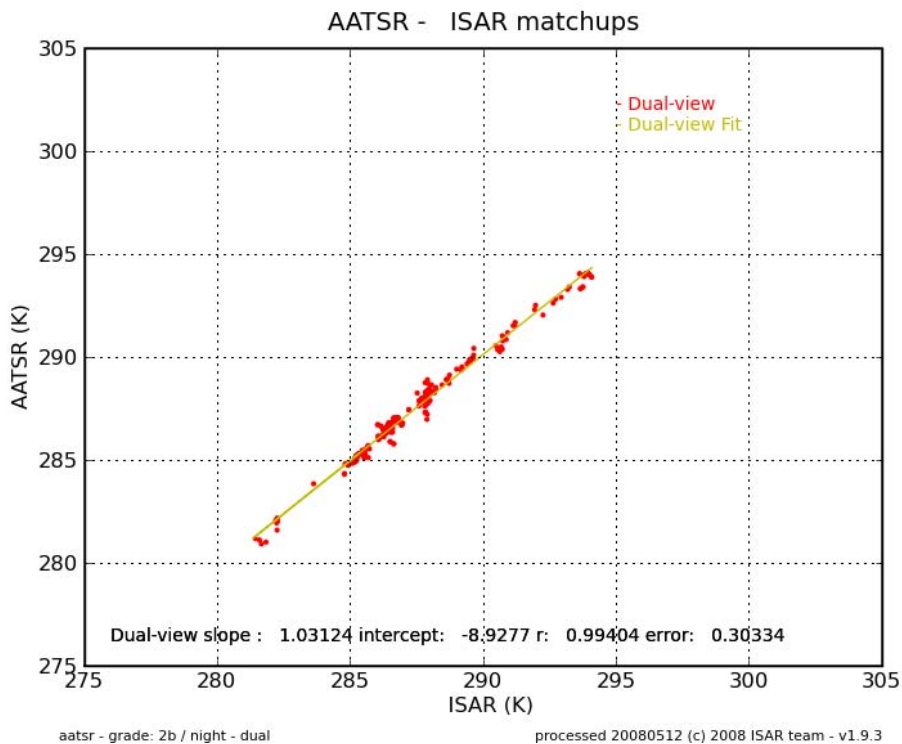
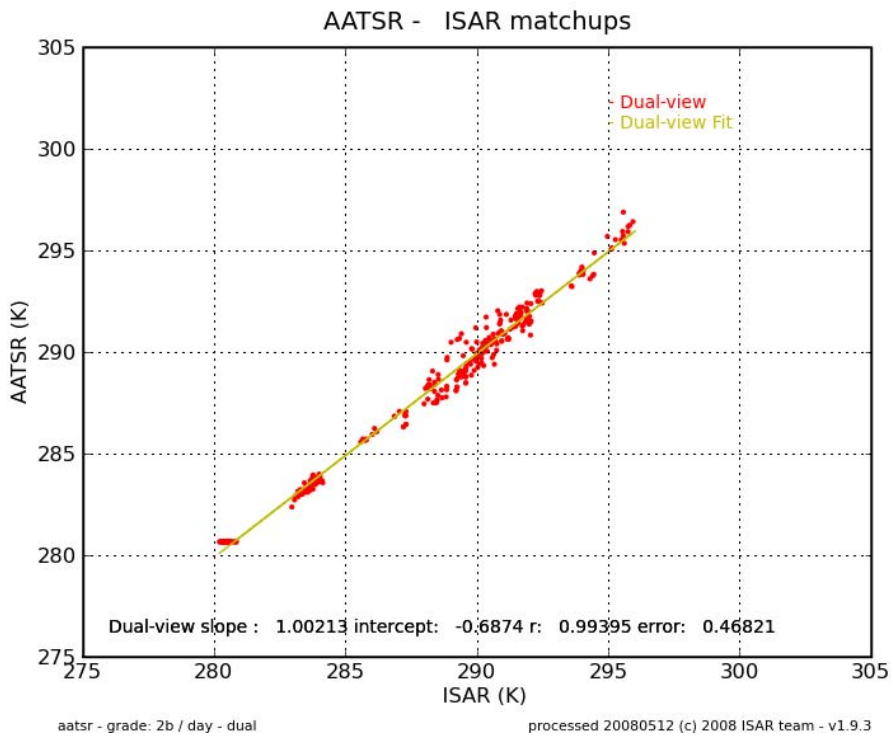


Figure 4-2: Scatter plot of the AATSR-SST dual-view retrievals and the Grade 2b coincident ISAR observations, for the period March 2004 to December 7th 2005. Top panel shows the 2-waveband retrievals (day) and the bottom panel shows the 3-waveband retrievals (night)

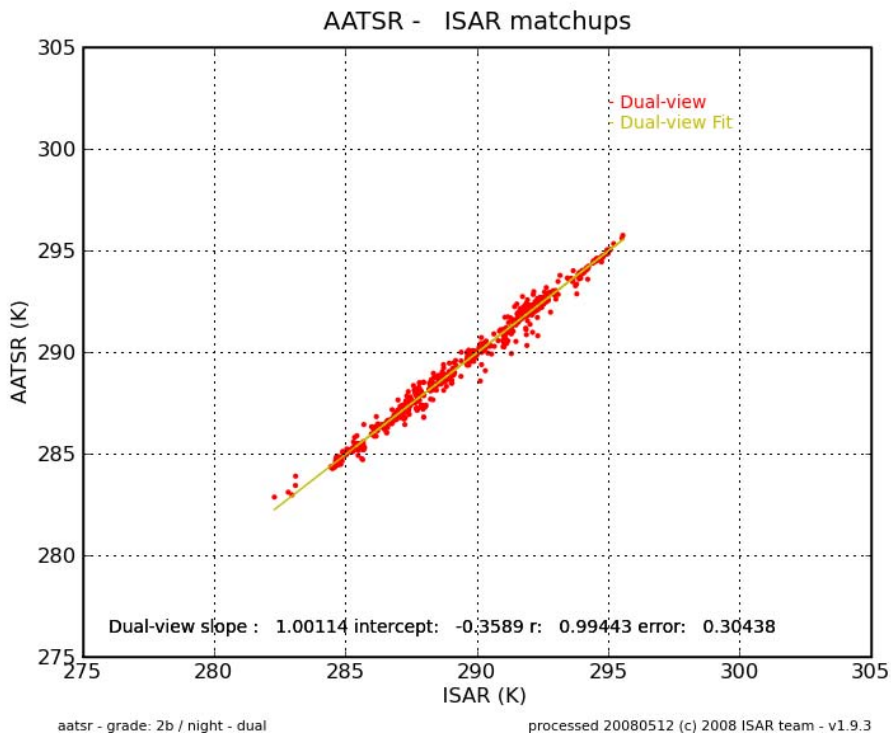
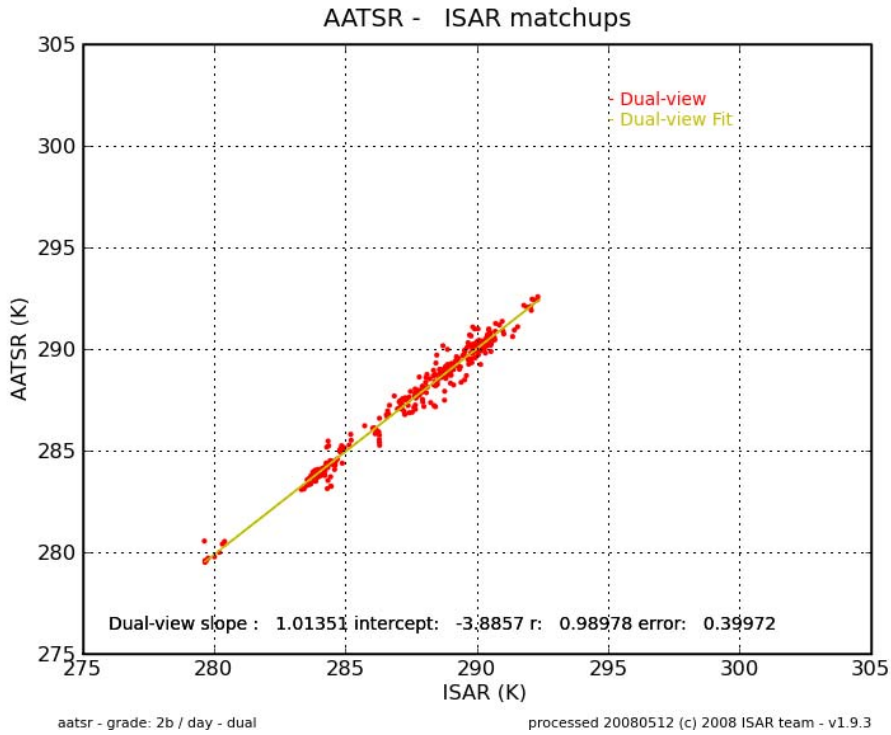


Figure 4-3: Scatter plot of the AATSR-SST dual-view retrievals and the Grade 2b coincident ISAR observations, for the period December 7th 2005 to January 2008. Top panel shows the 2-waveband retrievals (day) and the bottom panel shows the 3-waveband retrievals (night)

4.2 Nadir-view only algorithms

Although less important in relation to the international role of AATSR to provide an absolute standard SST dataset for use as a climate reference, it is still important to evaluate the performance of the SST products from the nadir-only algorithms. As in section 4.1 we first split the data in pre- and post-algorithm-change segments. These results are presented in tabular form in Table 4-4 and Table 4-5.

Table 4-4: Statistics for match-ups (AATSR nadir-only-view SST - ISAR) for Phase 1 before 7th December 2005, showing the bias and standard deviation, the number of matches, the number of overpasses from which they came, and the range of sea temperatures spanned by the match-up database.

Grade of coincidence	Mean bias, AATSR - ISAR	Standard deviation	No. of Matches	Overpass numbers	Min temp, °C	Max temp, °C
2 channel algorithm (N2)						
1	0.54	0.43	147	13	7.5	19.2
2a	0.43	0.68	287	24	7.5	19.7
2b	0.49	0.44	615	30	7.5	25.6
3	0.42	0.62	1165	42	7.5	25.6
4	0.37	0.62	3272	56	7.5	25.6
3 channel algorithm (N3)						
1	0.23	0.21	100	8	11.9	20.4
2a	0.06	0.36	230	16	8.2	21.3
2b	0.20	0.24	332	16	7.8	20.9
3	0.03	0.42	805	27	7.3	21.6
4	-0.02	0.49	2903	58	7.3	22.5

Table 4-5: Statistics for match-ups (AATSR nadir-only-view SST - ISAR) for Phase 1 after 7th December 2005 and all Phase 2, showing the bias and standard deviation, the number of matches, the number of overpasses from which they came, and the range of sea temperatures spanned by the match-up database.

Grade of coincidence	Mean bias, AATSR - ISAR	Standard deviation	No. of Matches	Overpass numbers	Min temp, °C	Max temp, °C
2 channel algorithm (N2)						
1	0.51	0.39	189	25	6.4	18.4
2a	0.58	0.68	482	43	6.4	20.4
2b	0.64	0.44	724	44	6.0	20.9
3	0.61	0.67	1569	57	5.6	21.4
4	0.73	0.82	4890	103	5.6	24.1
3 channel algorithm (N3)						
1	0.04	0.22	352	31	9.5	22.1
2a	-0.09	0.39	588	44	8.7	22.1
2b	0.02	0.23	1215	43	9.2	22.6
3	-0.11	0.44	2067	66	7.7	22.6
4	-0.14	0.47	6884	106	7.4	24.9

Here the picture is very different from the dual view retrievals. The 3-waveband single view algorithm seems to be performing quite well. With reference to the Grade 2b and Grade 1 match-ups it seems to have improved from a bias of around 0.2 K before the algorithm change to a bias less than 0.05 K and indistinguishable from zero. In both cases the standard deviation is less than 0.25 K. Like the dual view retrievals this is a remarkable result that points to the fine performance of AATSR.

However, the 2-waveband algorithm for the nadir-only view gives a bias that is 0.5 K or more. Moreover, according to the Grade 2b matches it seems to have grown to 0.64 K after the algorithm change. However, this difference may not be significant, when viewed against the variability in the bias between different match-up grades. The high bias is a result of a problem with the 2-waveband nadir-only algorithm that is well known to the AATSR validation team, and these data provide robust confirmation of the problem, as well as a dataset against which to test any algorithm changes.

For completeness, the statistics for the whole dataset, ignoring the algorithm change in December 2005, are presented in Table 4-6. It tends to show, as expected, biases somewhere between those in the other two tables, with slightly increased standard deviations.

Scatter plots for Grade 2b nadir-only match-ups are shown in Figure 4-4 and Figure 4-5 for before and after the 7th Dec 2005 algorithm change respectively. These illustrate graphically the degradation in performance of the 2-waveband algorithm (the upper plot of each figure) compared to the 3-waveband algorithm (the lower plot).

Table 4-6: Accumulated table of match-ups (AATSR nadir-only view SST - ISAR) for Phase 1 and Phase 2 showing the bias and standard deviation, the number of matches, the number of overpasses from which they came, and the range of sea temperatures spanned by the match-up database.

Grade of coincidence	Mean bias, AATSR - ISAR	Standard deviation	No. of Matches	Overpass numbers	Min temp, °C	Max temp, °C
2 channel algorithm (N2)						
1	0.52	0.41	336	38	6.4	19.2
2a	0.53	0.68	768	67	6.4	20.4
2b	0.57	0.45	1339	72	9.0	25.6
3	0.52	0.67	2745	95	5.6	25.6
4	0.58	0.76	8171	118	5.6	25.6
3 channel algorithm (N3)						
1	0.08	0.23	453	38	9.5	22.1
2a	-0.04	0.36	815	59	8.2	22.1
2b	0.06	0.24	1549	58	7.8	22.6
3	-0.08	0.45	2883	93	7.3	22.6
4	0.08	0.23	9790	38	7.3	22.6

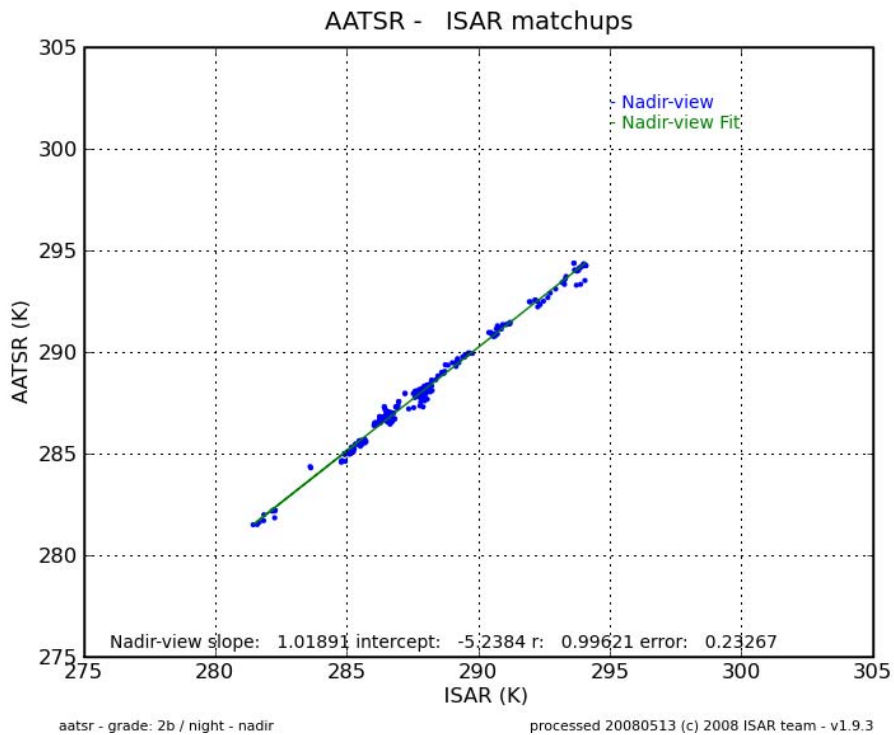
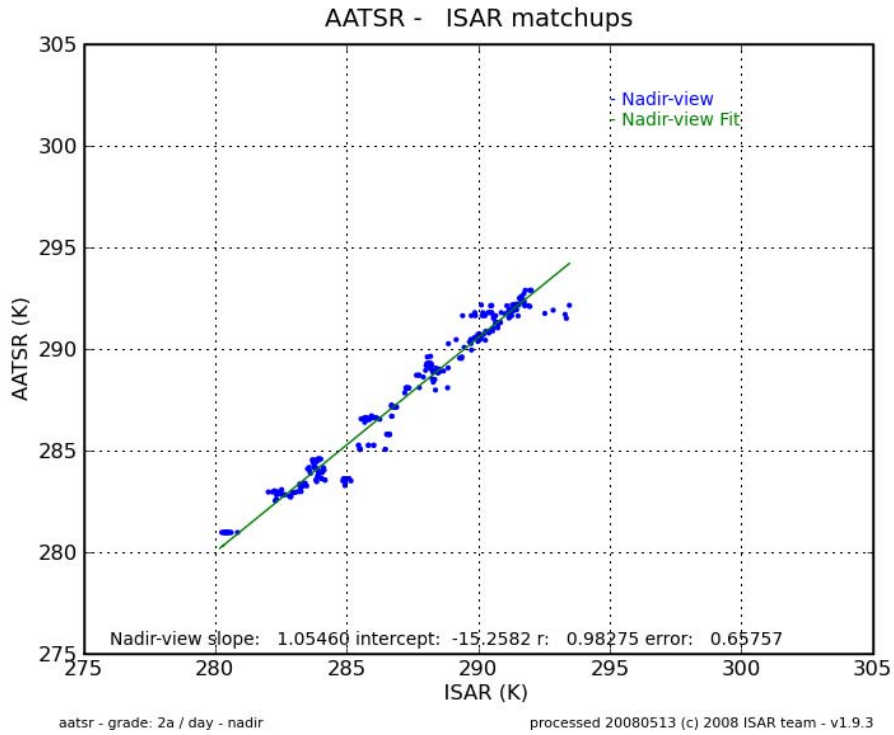


Figure 4-4: Scatter plot of the AATSR-SST nadir-only retrievals and the Grade 2b coincident ISAR observations, for the period March 2004 to December 7th 2005. Top panel shows the 2-waveband retrievals (day) and the bottom panel shows the 3-waveband retrievals (night).

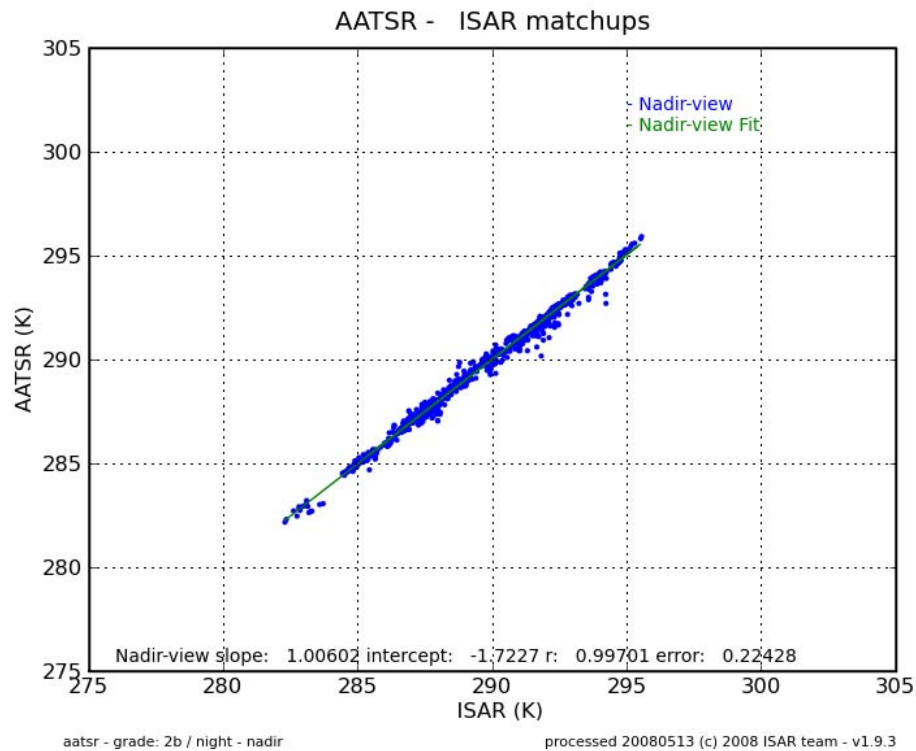
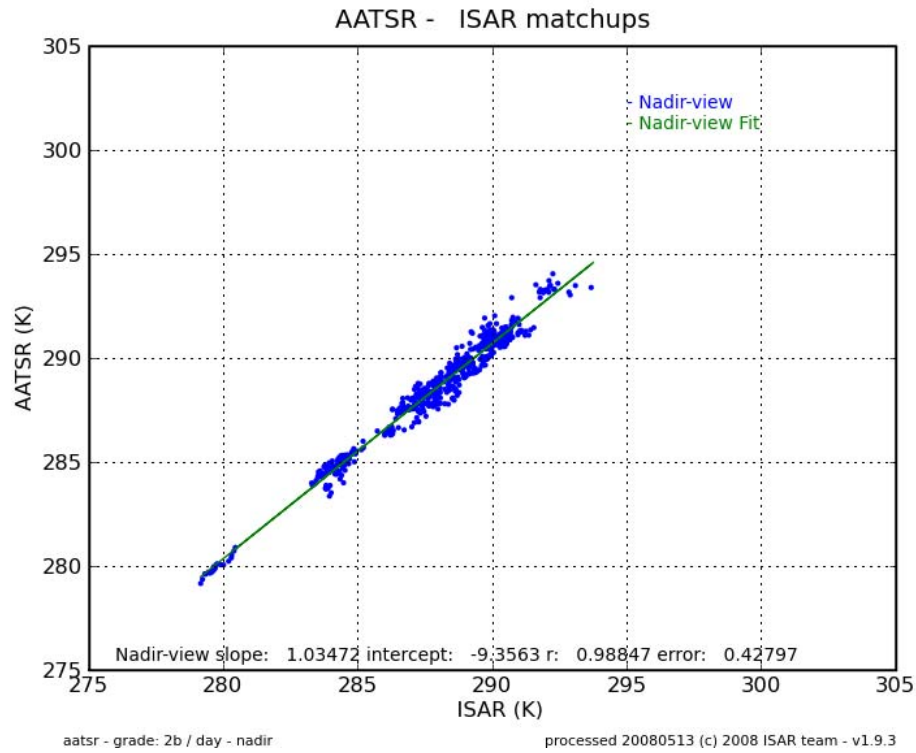


Figure 4-5 Scatter plot of the AATSR-SST nadir-only retrievals and the Grade 2b coincident ISAR observations, for the period December 7th 2005 to January 2008. Top panel shows the 2-waveband retrievals (day) and the bottom panel shows the 3-waveband retrievals (night).

4.3 Comparison between the performance of the different algorithms.

The histograms of the differences between ISAR and AATSR are shown in Figure 4-6 and Figure 4-7 for before and after the 7th Dec 2005 algorithm change respectively. The dual view histograms are shown in red on these plots and the nadir-only histograms in blue, while in each figure the upper plot shows the 2-waveband retrieval and the lower plot shows the 3-waveband retrievals. Since there are relatively small population numbers of Grade 2B match-ups, the histograms are not Gaussian and the peaks do not always correspond to the mean values. Therefore the mean differences have been plotted as vertical lines (yellow for the dual-view algorithm and green for the nadir-only algorithm) on the histograms.

The histograms confirm in visual form what is presented in the Tables in Sections 4.1 and 4.2. They show that the 2-waveband match-ups (for both dual and nadir-only retrievals) have a much larger standard deviation of nearly 0.5 K, implying that there are quite a lot of influential outliers in these data sets.

The histograms also show that the 3-waveband nadir-only algorithm is comparable in accuracy with both 2- and 3-waveband dual algorithms, which is consistent with the fact that there have been no major changes in stratospheric dust during the four years of the validations. However, the 2-waveband nadir-only algorithm has a significantly higher bias. This difference points to a discrepancy between the day time nadir-only retrievals and the night-time nadir-only retrievals.

When there is a considerable discrepancy between algorithms applied in the daytime and those applied at night, an obvious test to explore is how the 2-band algorithm performs at night. Normally it is used only in the day time when the 3-band algorithm cannot be applied, and is not a standard product at night. However, the Validation Scientist was able to provide 2-band night time AATSR data corresponding to the ISAR match-ups from 60 daytime and 60 night time overpasses. These included both dual view and nadir-only SST retrievals.

The resulting differences from ISAR are shown in Table 4-7 for grades 1 and 2B match-ups only. Comparing the 2-band daytime with the 2-band night time results for the dual-view algorithm (upper half of the table the bias values are identical to two decimal places, and the standard deviation is similar, although it is lower for the night time orbits when there were a larger number of match-ups.

For the nadir-only view the result is very similar too. The much larger bias (for this set of orbits it was over 0.7 K) is the same for both day and night for Grade 2b match-ups and similar for Grade 1. This demonstrates clearly that the problem with the 2-waveband nadir-only algorithm is not associated with applying the algorithm in daytime.

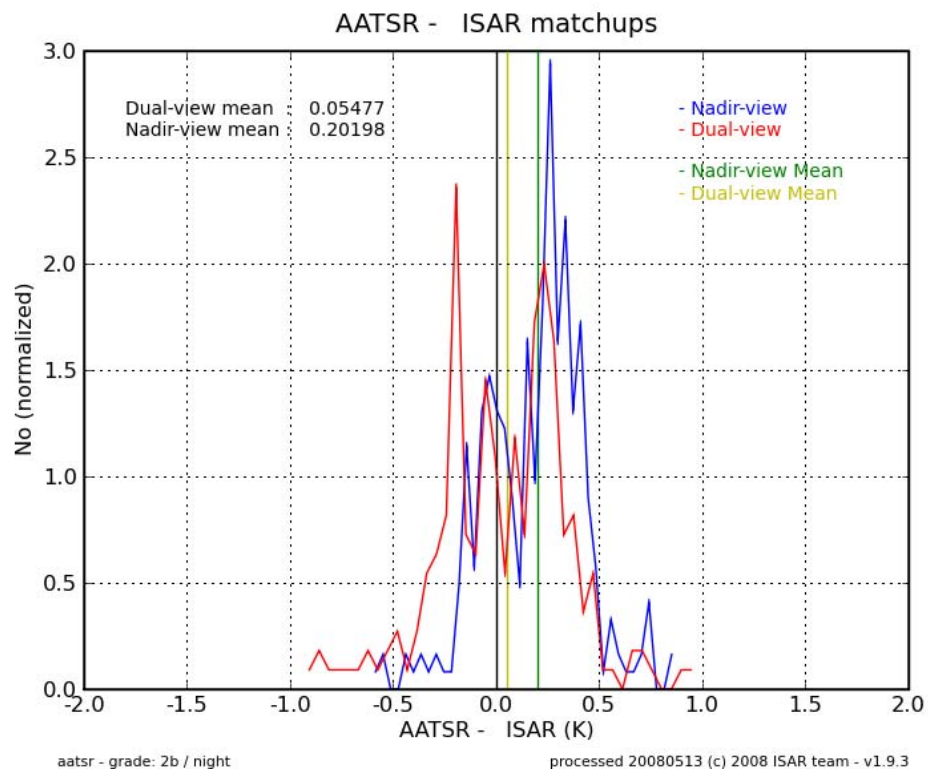
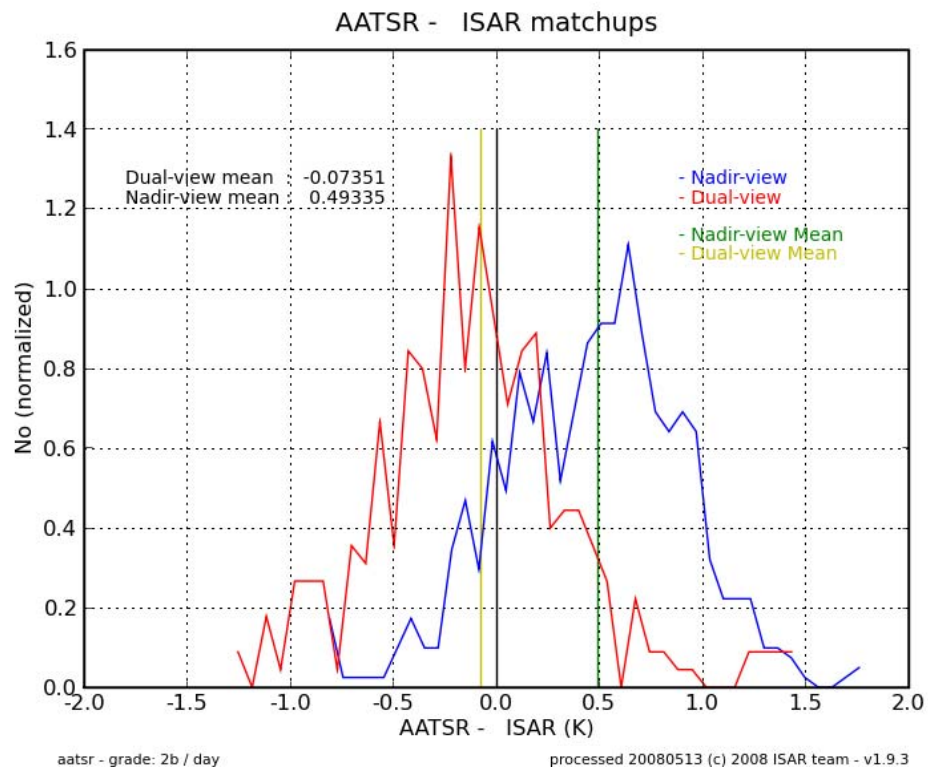


Figure 4-6: Histogram of the differences between the AATSR-SST retrievals (both dual -view and nadir-only algorithms) and all the Grade 2b coincident ISAR observations, for the period March 2004 to December 7th, 2005. The top panel shows the 2-waveband (daytime) retrievals and the lower panel the 3-waveband (night) retrievals.

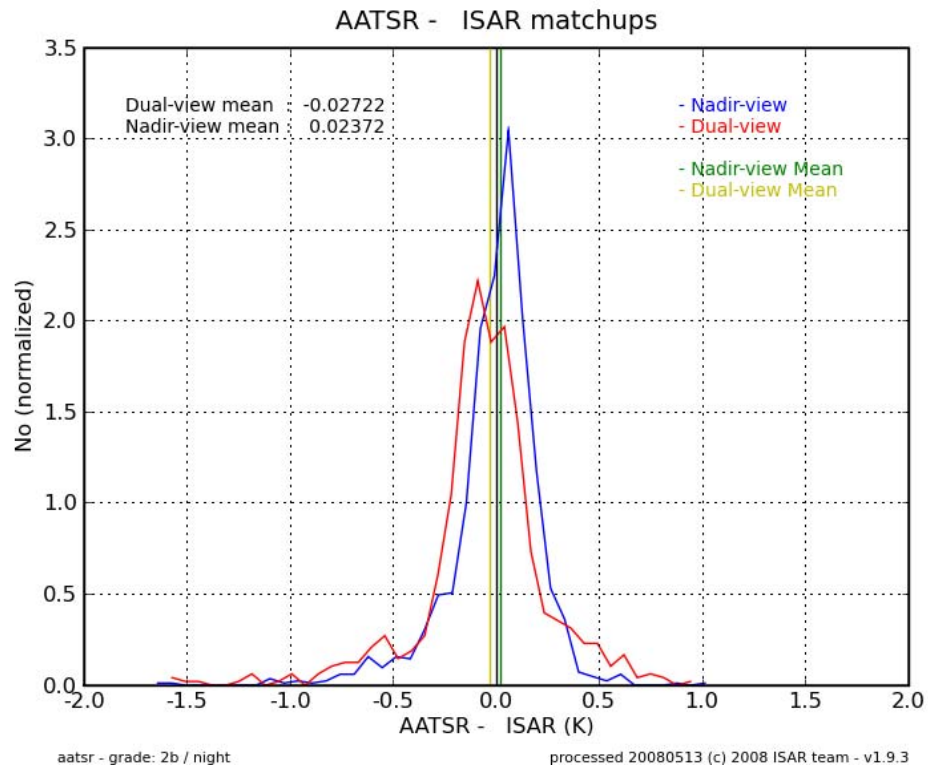
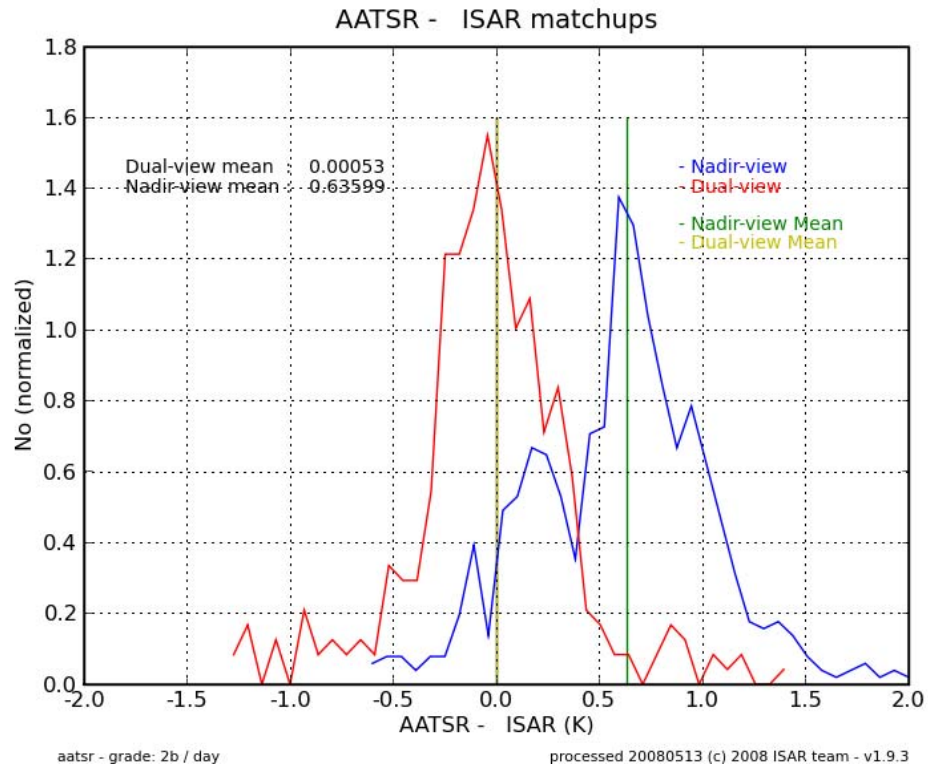


Figure 4-7: Histogram of the differences between the AATSR-SST retrievals (both dual -view and nadir-only algorithms) and all the Grade 2b coincident ISAR observations, for the period from December 7th, 2005 to January 2008. The top panel shows the 2-waveband (daytime) retrievals and the lower panel the 3-waveband (night) retrievals.

Table 4-7: Special comparison between day-time and night-time evaluations of the dual and nadir 2-waveband algorithms

Grade of coincidence	Mean bias, AATSR - ISAR	Standard deviation	No. of Matches	Overpass numbers	Min temp, °C	Max temp, °C
Dual view 2 channel algorithm daytime retrievals						
1	0.03	0.40	201	60	6.4	19.2
2b	0.04	0.49	819	60	6.0	23.8
Dual-view 2 channel algorithm night time retrievals						
1	0.03	0.38	336	60	9.1	23.1
2b	0.04	0.34	1199	60	8.5	23.1
Nadir-only view 2 channel algorithm daytime retrievals						
1	0.71	0.45	285	60	6.4	19.2
2b	0.76	0.46	1111	60	6.0	23.8
Nadir-only view 2 channel algorithm night time retrievals						
1	0.74	0.38	379	60	9.1	23.1
2b	0.76	0.40	1327	60	8.5	23.1

5. Ancillary Studies

5.1 A quality flagging scheme for validation match-ups

This subsection reports on the outcome of the ancillary study to develop a new method for flagging the quality of match-ups according to how likely they are to be comparing like with like. The study is described in detail in a separate report. Here the method is briefly outlined and then the match-up results shown in section 4 are re-presented when stratified in terms of the new quality flags.

5.1.1 Theoretical approach to error minimisation

The purpose of the validation of satellite measurements is to quantify the error of the satellite measurement, E , defined as

$$E = V_S - T$$

Where V_S is the satellite measurement of a property, in this case SST, and T represents the true value of that property, as averaged over the area represented by the pixel to which V_S refers. In practice we do not know T but instead an *in situ* validation measurement, V_I , is made as an approximation to T . The extent to which the *in situ* measurement fails to represent a pixel-area average of the SST, at the precise instant and over the exact area viewed by the satellite sensor, can be described as the match-up error, E_{MU} , where $E_{MU} = V_I - T$. Thus the comparisons between the satellite and *in situ* measurements performed during validation produce errors which are the sum of the actual satellite error and the match-up error, i.e.

$$V_S - V_I = E + E_{MU}$$

This means that the validation process itself may artificially inflate the magnitude of the satellite measurement error if E_{MU} is not negligible. The reason for grading the match-ups as 1 to 4 in the rather coarse way explained in 3.3.1 is because it may be expected that E_{MU} should be smaller when the space-time mismatch between the *in situ* and the satellite measurement is small, as for Grade 1 match-ups.

The purpose of the ancillary study in WP700 of Phase 2 was to explore the factors contributing to E_{MU} and thereby develop a means of estimating its relative magnitude for every match-up data pair, using data available from the satellite or the ISAR. The objective was then to attach a quality value, Q , to each match-up pair according to whether its expected E_{MU} would be smaller (leading to high quality matches) or larger (leading to lower quality matches). The ideal is to identify match-ups of the highest quality for which E_{MU} is negligibly small, and a rank of lower quality values for which E_{MU} becomes progressively larger. After theoretical analysis and some trial and error, the following method was developed, refined and adopted.

We can write with general applicability for validating a variety of satellite data:

$$E_{MU} = E_S + E_T + E_M + E_P + E_Z,$$

where E_S is the spatial mismatch error, E_T the temporal mismatch error E_M the instrument error of the *in situ* sensor, E_P the point-in-area sampling error (this is the error associated with using a single or a few point samples from a ship to represent the average of a variable over the whole pixel area represented by a satellite measurement) and E_Z is the sampling depth error (if the *in situ* measurement is made at a different depth in the water column than is sampled by the satellite).

In the particular case of the ISAR, these components, E_x , of the match-up error can be estimated from available knowledge by evaluating indicators, I_x , as follows:

E_S is represented by I_S which is the product of the offset distance (between the ISAR sample and the AATSR pixel) and the maximum spatial gradient of temperature (derived by fitting a plane to a 9×9 block of AATSR pixels ignoring cloud), without reference to the relative orientation of the offset or the gradient.

I_S is a temperature difference with units of K.

E_T is represented by I_T which is the product of the offset time (between the ISAR sample and the AATSR overpass) and the mean temporal trend of temperature from 1 hr of the ISAR record.

I_T is a temperature difference with units of K.

E_M is treated differently. Because of the way the ISAR measurements of brightness temperature are internally calibrated and externally validated, there is no grading of measurement quality. Data are either within specification (± 0.1 K) or rejected. This places a noise baseline of 0.1 K on all estimates of the satellite error, E . However, when the ISAR estimates skin temperature it measures the sky radiance to allow for surface reflected radiation. Should the sky view be of cloud, this will introduce an error which must be quantified. For this we specify an indicator I_{Sky} which is simply defined as the brightness temperature of the Sky view of ISAR.

I_{Sky} is an absolute temperature with units of K.

E_P derives essentially from the sub-pixel scale variability of the SST field, which is difficult to quantify precisely from available observations. In practice it is estimated in two different ways, represented by two indicators:

I_{P1} is based on the temperature variance of a 9×9 block of AATSR cloud-free pixels, multiplied by the χ^2 (95%) confidence interval to produce the explained variance.

I_{P2} is based on the temperature variance of 1 hr of the ISAR temperature record, scaled by the χ^2 (95%) confidence interval

The units of I_{P1} and I_{P2} are $(K)^2$.

E_Z should be eliminated by measuring the skin temperature and is not considered.

For every match-up, the indicators defined above can be calculated from data gathered by the ISAR and ancillary sensors.

Four quality flags, Q_x , between 0 and 3 have been created in respect of each indicator, as shown in Table 5-1 where each row represents a particular indicator. The indicator values are thresholds corresponding to the maximum value permitted for an indicator if it is to be assigned the quality flag numbered at the top of the column. Each indicator is first tested against the Q3 thresholds. If this is exceeded the Q2 threshold is tested etc. until the threshold is satisfied. Q0 corresponds to all cases that fail to meet any threshold. The thresholds have been determined empirically.

Table 5-1: Threshold values of indicators, I_x , for assigning quality flags Q_x .

Quality flag	Units	0	1	2	3
Q_{P1}	K^2	No threshold	0.3	0.1	0.035
Q_{P2}	K^2	No threshold	0.3	0.1	0.035
Q_T	K	No threshold	0.6	0.2	0.05
Q_S	K	No threshold	0.25	0.07	0.025
Q_{Sky}	K	No threshold	280	260	240

Once the five separate Q_x flags have been assigned to a match-up value, the overall quality value, Q , is set as the minimum of the five separate flags, i.e.

$$Q = \text{Min}\{Q_{P1}, Q_{P2}, Q_T, Q_S, Q_{Sky}\}$$

Thus for a match-up to be assigned a quality value of 3, all the indicators must be lower than the thresholds in the right hand column of the table.

5.1.2 AATSR - ISAR Match-ups stratified by Match-up Quality Value

The results for the dual-view performance, previously shown in Table 4-3 when stratified by the coincidence grading scheme are presented again in Table 5-2, this time stratified in terms of the Quality Value. The results are very encouraging from two perspectives

Firstly, the way in which the standard deviation gets progressively smaller as the size of the dataset is reduced by the elimination of match-ups having lower quality values implies that the new method developed in WP700 of phase 2 is working well. Whilst the thresholds were tuned in order to achieve this result, the tuning was done for the data from a single deployment only. That the thresholds appear to be applicable across all deployments suggests that they can be used universally, at least for the region traversed by the *Pride of Bilbao*.

Table 5-2: Match-up statistics for all AATSR dual-view SST retrievals compared with ISAR data during March 2004 to February 2008, stratified by quality value Q

Quality filter	AATSR - ISAR temp difference, K		Total number of sampled:		Temp range, °C		Time difference, minutes		Distance offset, km	
	Mean	St. Dev.	Matches	O'pass	Min,	Max,	Min,	Max,	Min	Max
2-waveband SST retrievals										
0	-0.03	0.62	909	67	6.4	23.7	0.2	120	0	24.4
1	-0.03	0.31	423	43	6.4	23.3	0.3	120	0	24
2	-0.05	0.21	202	20	7.5	22.2	0.6	120	0	24
3	-0.08	0.19	55	10	9.9	18.2	0.6	120	0	9
3-waveband SST retrievals										
0	-0.04	0.40	1378	68	7.7	22.54	0.3	120	0	26.2
1	0.01	0.24	775	48	11.2	22.2	0.3	120	0	24.2
2	-0.03	0.18	343	35	11.3	21.9	0.3	120	0	19.9
3	-0.01	0.11	66	13	11.5	20.9	0.8	103	0	19.9

Secondly, and more pertinent to the primary objective of the contract, the fact that the standard deviation for the highest quality match-ups reaches a value as low as 0.11 for the 3-waveband retrievals demonstrates just how good the AATSR performance really is. It should be noted that the basis for restricting the match-ups allowed into the exclusive Quality Value 3 is a set of indicators associated with the natural variability of the wider SST field and thus eliminating situations when the ISAR and AATSR are not observing the same "sea truth". When that uncertainty is removed, the only factor left to contribute to the error is the performance of the AATSR and the ISAR themselves. Since the ISAR is validated to 0.1 K, the implication is that every sample of the AATSR dual view is at least as accurate as the ISAR.

Based on the standard deviation of the Quality Value 2, which widens the number of samples to more than 500, these results confirm that we can have confidence that every SST dual view product pixel delivered from AATSR has an individual absolute uncertainty of less than 0.21 K. Repeated measurements can establish SST to an accuracy better than 0.1 K.

When the method is applied to the nadir-only retrievals from AATSR, as shown in

Table 5-3, the result for the 3-waveband retrieval is similar to the dual view. The standard deviation for Quality Value 3 is as low as 0.12 K, although there is a bias of 0.10 K. Thus for measurements over the validated region, the application of a bias adjustment of 0.1 K should lead to an absolute accuracy of about 0.1 K to AATSR nadir view night time data.

For the 2-waveband view, the contrast is significant. The fact that the Quality Value 3 data cannot reduce the standard deviation below 0.33 K, in contrast with the other cases, suggests that this is the level of uncertainty within the AATSR data product itself, and is not primarily associated with the match-up process nor the

Table 5-3: Match-up statistics for all AATSR nadir-only SST retrievals compared with ISAR data during March 2004 to February 2008, stratified by quality value Q

Quality filter	AATSR - ISAR temp difference, K		Total number of sampled:		Temp range, °C		Time difference, minutes		Distance offset, km		
	Q ≥	Mean	St. Dev.	Matches	O'pass	Min,	Max,	Min,	Max,	Min	Max
2-waveband retrievals											
0	0.49	0.68	2658	99	6.0	24.0	0.2	>720	0	24.7	
1	0.57	0.42	1166	73	6.0	24.0	0.2	120	0	23.1	
2	0.59	0.36	491	39	6.4	22.9	0.2	120	0	22.4	
3	0.68	0.33	140	22	9.6	21.4	0.4	120	0	22.4	
3-waveband SST retrievals											
0	-0.09	0.46	2748	112	7.3	22.8	0.2	8732	0	26.1	
1	0.04	0.22	1491	62	7.9	22.4	0.2	120	0	23.9	
2	0.10	0.17	636	49	11.5	22.1	0.2	120	0	23.7	
3	0.10	0.12	137	21	11.6	21.0	0.2	120	0	23.7	

5.2 Study of skin-bulk processes

The ancillary study performed within WP800 aimed to use the opportunity afforded by a considerable database of skin (ISAR) and bulk (SeaBird hull thermometer) measurements of SST to determine whether a relationship exists between the two. The practical question to be addressed is whether it is feasible to use hull mounted thermometers (that are widely available) as a proxy for true

skin measurements (that are very sparse) for the validation of satellite SST measurements derived from skin temperature.

The study involved the addition of further hull thermistors at different depths below the water line and on opposite sides of the vessel. It also made use of data from a thermometer installed on a towed continuous plankton recorder which is deployed from time to time from the *Pride of Bilbao*. The details of the study are written in a separate report.

The broad conclusion was that it is extremely difficult to use hull thermometry as a proxy for skin SST measurements. Although there are circumstances when depth temperature measurements can be stably related to skin temperature measurements, this depends on careful calibration, not only of the thermometers themselves but of the particular installation of the hull thermometer. Relevant factors include the depth of the hull sensor, the ambient temperature inside the hull relative to the sea temperature, the speed of the vessel, the direction of the wind, and so on. As a result we found that the ISAR instrument produced more accurate and repeatable temperature measurements than any of the other temperature sensors. It is apparent that in order to use a substitute depth temperature measurement for validating satellite skin temperature observations it would first require careful experiments using a radiometer to individually characterise the skin-hull thermometer characteristics unique to each vessel. Even then the results would have much poorer reliability than using a ship-borne radiometer. While this issue deserves further scientific study, we conclude that it is much simpler and more reliable to install a bridge mounted radiometer for ship-of-opportunity monitoring of SST for satellite validation.

6. Conclusion

6.1 Achievements of the project

The completion of another two years of operational SST_{skin} data acquisition on the *Pride of Bilbao* for validation of AATSR has not only shown the continuing effectiveness of the ISAR but also the excellent stability and accuracy of the AATSR SST measurements. During the last four years of operation (phase 1 and phase 2 of this project), a total of 1642 match-up pairs of dual view satellite retrievals and *in situ* observations were acquired, measured within 1 km and 2 hours of each other, corresponding to 130 individual satellite overpasses. The change in AATSR SST retrieval coefficients in December 2005 showed very little change in the dual view SST retrieval, however the nadir view SST retrieval shows higher biases for the two channel data after the coefficient change with similar standard deviations before and after the AATSR SST coefficient change. The higher bias of the AATSR nadir-only view day-time two channel SST validation was investigated by using two channel day and night-time AATSR nadir view data and it was found that the most likely cause for the bias is the AATSR two channel nadir view retrieval algorithm.

A new method for the estimation of the match-up error was developed and has shown very good initial results. This method does minimize the error introduced by the match-up process itself and therefore stratifies the match-up data set, not by arbitrary temporal or spatial limits but by an objective estimate of the error introduced by matching data which does not coincide perfectly in time and space. The results for the best quality 66 validation match-up pairs for the AASTR dual view three channel SST from 13 individual satellite overpasses give a bias very close to 0 and a very low standard deviation of 0.11K.

The investigation into using hull mounted thermistors as a proxy for the SST_{skin} measurements and subsequently for the validation of AATSR data, showed that although this is possible it would not show the true excellence of the SST data acquired by AATSR because of the large errors associated with the residual uncertainties in such a comparison.

6.2 Requirement for ongoing work

It is now widely recognised that the ATSR class of sensors (ATSR-1, ATSR-2 and AATSR) provide a stable and probably the most accurate source of sea surface temperature (SST) available as a baseline measurement for climate change monitoring and research. The GHRSSST-PP science team explicitly recognises the role of AATSR on Envisat to provide a reference standard needed to underpin a stable long-term SST climate product. Although the AATSR is independently calibrated by on-board reference blackbodies, it requires an ongoing programme of validation against *in situ* measurements to demonstrate that the SST products it delivers meet the AATSR science requirements. Without such a validation programme the usefulness of AATSR SST data as a quality

standard for other systems is open to question. For that reason it is appropriate that, having procured the sensor initially, Defra should maintain an ongoing validation programme for AATSR SST products, especially as the ISAR project is currently the only continuously operational SSTskin measurement programme worldwide.

The experience we have gained with the ISAR instrument over the last four years not only gives us confidence that we can operate the ISAR successfully for a further two years, but encourages us to believe that this technique deserves to be extended to validate satellite SST retrieved from other sensors and to cover much wider geographical areas for better validation coverage.

Appendix A Revised internal calibration algorithm

Changes were made to the calibration algorithm that converts raw counts from the instrument into SST retrievals.

The baseline calibration method must allow for the fact that, although the radiometer field of view is constrained by the field stop in front of the scan drum mirror, it is never possible to eliminate all stray radiation emitted by, or reflected from, inside the radiometer. Thus calibration of the externally viewed radiances is based on comparing the detector signal when viewing outwards to that when viewing the calculated radiance from an internal black body cavity of known temperature, assumed to fill the same field of view as the external aperture. If we assume that a large proportion, p , of the radiance reaching the detector is from the defined field of view, then the total radiance, L_d , reaching the detector when viewing a target with radiance L_T must be:

$$L_d = pL_T + (1-p)L_{amb} \quad (1)$$

where L_{amb} is the ambient stray radiation inside the sensor. We further assume that the instrument signal (that is, its output in counts, C) are proportional to radiance over the range of brightness temperatures of concern to the ISAR measurements. Thus we may write

$$C = g.L_d \quad (2)$$

where g is the internal gain of the detector in counts per radiance units.

For each measurement cycle the system records the average signal, C_{sea} and C_{sky} , when the scan mirror points the field of view through the external aperture towards the sea or the sky. It also points internally to the ambient black body (bb1) and the heated blackbody (bb2) recording average counts of C_{bb1} and C_{bb2} respectively. From these records we can calculate :

$$X_{sea} = \frac{C_{sea} - C_{bb1}}{C_{bb2} - C_{bb1}} \quad \text{and} \quad X_{sky} = \frac{C_{sky} - C_{bb1}}{C_{bb2} - C_{bb1}}. \quad (3a, 3b)$$

Substitution of (2) and (1) in (3a) eliminates the unknowns p , g and L_{amb} , yielding:

$$X_{sea} = \frac{L_{sea} - L_{bb1}}{L_{bb2} - L_{bb1}} \quad \text{and hence}$$

$$L_{sea} = X_{sea}L_{bb2} + (1 - X_{sea})L_{bb1}. \quad (4)$$

A similar equation expresses the sky radiance L_{sky} in terms of X_{sky} . As long as p , g and L_{amb} remain constant within a measurement cycle of one to two minutes, this approach allows any gradual drift in

p , g and L_{amb} to be accommodated without affecting the accuracy of the retrieved target radiance, that is the sea view radiance, the sky radiance or any other target presented to the radiometer such as the laboratory calibration black body. It allows for some degradation of the scan mirror surface which may reduce direct reflection and increase emission by the mirror surface itself so that the proportion $(1-p)$ of stray radiation increases. As long as the effect is identical for each view (sea, sky and black bodies) the retrieval of the radiance from external targets using Eqn.4 is not compromised.

While the laboratory calibration tests before and after each deployment confirmed the general robustness of this approach, it also showed that the degradation occurring by the end of a three month deployment was leading to marginal performance within the ± 0.1 K specification of the ISAR. The main source of the problem appears to be in estimating the absolute radiances leaving each of the black bodies and reaching the scan drum aperture. These are needed to evaluate Eqn. 4, and are calculated using:

$$L_{BB} = \varepsilon B_B(T_{bb}) + (1 - \varepsilon) B_B(T_{amb}) \quad (5)$$

where L_{BB} is the radiance leaving the black body in the field of view of the radiometer, ε is the effective emissivity of the blackbody and B_B is the bandwidth adjusted Planck function for the detector bandwidth, evaluated for the blackbody temperature (T_{bb}) or the ambient temperature (T_{amb}) internally within the ISAR, both of which are measured to a high accuracy by thermistors. The emissivity is a measure of the non-blackness of the blackbody integrated across the field of view of the radiometer through the scan-drum aperture. This may encounter the edge of the black body aperture, even when the scan mirror is in a pristine state at the start of a deployment. Thus the heated black body, when viewed through the field stop, is probably not perfectly uniform, but may have a slightly cooler annular region around its circumference. To allow for this small effect, the emissivity was estimated in the original algorithm to be 0.9993, and the use of this value is confirmed by the pre-deployment laboratory calibrations.

When the scan mirror degrades, not only does it reduce the reflected signal as discussed above, but it is also likely to cause some scattering of the reflected radiation. This means that the radiometer now receives some radiation scattered into its field of view from a wider range of angles beyond the mirror than it does when the mirror is pristine. The surfaces inside the ISAR that determine the magnitude of this scattered radiation are different for different settings of the scan drum, that is the extra stray radiation is different for the external view and each of the black body views. Since the additional radiation will be mostly at the ISAR's ambient temperature, the effect is accommodated largely by a further change in p , but this does not allow for any small changes between different scan drum pointing directions. In particular, when viewing the heated black body, the integrated radiance from the new spread of directions associated with the scattering surface is likely to be reduced because it includes regions around the cooler flange of the scan drum aperture. To allow for this factor and prevent it from degrading the radiance calibration requires a small reduction of the effective emissivity of the black bodies, ε in Eqn. 5.

Trial and error showed that reducing ε by a small amount readily achieved a very good match to the post-deployment laboratory calibration, even when the mirror was badly degraded. That discovery by itself could not provide a practical adjustment to ε during a deployment. What is required is to define $\varepsilon = \varepsilon_0 - \varepsilon'$ where ε_0 is the pre-deployment effective emissivity set at 0.9993, and then to find a means to vary ε' continuously as an objective response to the actual degradation of the mirror. Fortunately the mirror response is readily monitored by evaluating a nominal gain factor, G , where:

$$G = \frac{C_{bb2} - C_{bb1}}{L_{BB02} - L_{BB01}} \quad (6)$$

and the black body radiances are evaluated using the initial emissivity value $\varepsilon_0 = 0.9993$. That is:

$$L_{BB0} = \varepsilon_0 B_B(T_{bb}) + (1 - \varepsilon_0) B_B(T_{amb}) \quad (7)$$

As the mirror degrades during a deployment, ρ increases so less of the radiance emitted by the hot black body reaches the detector (see Eqn. 1), so that (from Eqn 2) C_{bb2} is reduced and thus G decreases as a direct measure of the mirror degradation. [Note that G is also used as a diagnostic decision tool for aborting a deployment earlier than planned if a sudden major mirror degradation is noted.] At the same time, the use of $\varepsilon = \varepsilon_0$ in (5) means the black body emission is slightly overestimated when the mirror degrades, which further reduces G .

Thus the difference between G_0 (the value of G evaluated from the pre-deployment calibration) and the subsequent value of G at every measurement cycle of the deployment can serve as an indicator of ε' . A simple linear relationship, $\varepsilon' = f_W(G_0 - G)$, was found to be applicable, with a weighting factor, f_W , of 0.45. Thus

$$\varepsilon = \varepsilon_0 - f_W(G_{precal} - G). \quad (8)$$

The new radiance retrieval algorithm evaluates (7) and then (6), in order to obtain ε from (8) at every measurement cycle. The evaluation of Eqn. 3 is unchanged from the original algorithm, but then the radiance is derived using the result of (8) in (5) to calculate the correct black body radiance to enter in (4) which delivers the desired target radiance. We have also modified (5) slightly by using measurements of the temperature of the flange surrounding the black body cavity in place of T_{amb} in the second term on the r.h.s.

The experience of applying the methods to most of the deployments from Phase 1 and Phase 2 showed that the selection of $f_W = 0.45$ was applicable to them all. The new algorithm always led to the post deployment laboratory calibration being almost identical to the pre-deployment calibration. These results were presented in the July 2007 Monthly Management Report. The theoretical hypothesis, presented here to explain the problem, is thus supported by the empirical consistency of the results. However empirical tests will be needed to confirm whether $f_W = 0.45$ remains applicable for new or refurbished ISARs if changes of internal geometry affect the heated black body view.

Appendix B Data acquired by ISAR

Note for all tables in Appendix B: The file name ending in *ISAR5C_002* (or *003*) is the ISAR instrument record, the file name ending with *Wind* is the anemometer record, the file name ending *Vaisala* is the Vaisala dew point thermometer record and the file name ending *MPack* is the combined Seabird hull thermometer and FerryBox minipack record. The filename ending H THERM contains the logged data from the additional hull thermistors.

B.1 Data records for D10: ISAR-002, 21 February to 10 May 2006

Recording period	Data files acquired
21/02/06 - 27/02/06	20060221T174010Z_20060227T225336Z.ISAR5C_002 20060221T174010Z_20060227T225336Z.Wind
28/02/06 - 09/03/06	20060228T000410Z_20060309T091256Z.ISAR5C_002 20060228T000410Z_20060309T091256Z.Wind 20060228T000410Z_20060309T091256Z.Vaisala 20060228T000410Z_20060309T091256Z.MPack
09/03/06 - 10/04/06	20060309T093529Z_20060410T174644Z.ISAR5C_002 20060309T093529Z_20060410T174644Z.Wind 20060309T093529Z_20060410T174644Z.Vaisala 20060309T093529Z_20060410T174644Z.MPack
10/04/06 - 19/04/06	20060410T183258Z_20060419T154510Z.ISAR5C_002 20060410T183258Z_20060419T154510Z.Wind 20060410T183258Z_20060419T154510Z.Vaisala 20060410T183258Z_20060419T154510Z.MPack
19/04/06 - 10/05/06	20060419T164212Z_20060510T170849Z.ISAR5C_002 20060419T164212Z_20060510T170849Z.Wind 20060419T164212Z_20060510T170849Z.Vaisala 20060419T164212Z_20060510T170849Z.MPack

B.2 Data records for D11: ISAR-003, 10 May to 9 August 2006

Recording period	Data files acquired
10/05/06 - 16/05/06	20060510T175613Z_20060516T164703Z.ISAR5C_003 20060510T175613Z_20060516T164703Z.Wind 20060510T175613Z_20060516T164703Z.Vaisala 20060510T175613Z_20060516T164703Z.MPack
16/05/06 - 12/06/06	20060516T170520Z_20060612T195000Z.ISAR5C_003 20060516T170520Z_20060612T195000Z.Wind 20060516T170520Z_20060612T195000Z.Vaisala 20060516T170520Z_20060612T195000Z.MPack
15/06/06 - 21/06/06	20060615T113144Z_20060621T175219Z.ISAR5C_003 20060615T113144Z_20060621T175219Z.Wind 20060615T113144Z_20060621T175219Z.Vaisala 20060615T113144Z_20060621T175219Z.MPack 20060615T113144Z_20060621T175219Z.HTHERM
21/06/06 - 27/06/06	20060621T190638Z_20060627T165041Z.ISAR5C_003 20060621T190638Z_20060627T165041Z.Wind 20060621T190638Z_20060627T165041Z.Vaisala 20060621T190638Z_20060627T165041Z.MPack 20060621T190638Z_20060627T165041Z. HTHERM
27/06/06 - 18/07/06	20060627T170426Z_20060718T164529Z.ISAR5C_003 20060627T170426Z_20060718T164529Z.Wind 20060627T170426Z_20060718T164529Z.Vaisala 20060627T170426Z_20060718T164529Z.MPack 20060627T170426Z_20060718T164529Z.HTHERM
18/07/06 - 09/08/06	20060718T170706Z_20060809T142500Z.ISAR5C_003 20060718T170706Z_20060809T142500Z.Wind 20060718T170706Z_20060809T142500Z.Vaisala 20060718T170706Z_20060809T142500Z.MPack 20060718T170706Z_20060809T142500Z.HTHERM

B.3 Data records for D12: ISAR-002, 9 August to 6 November 2006

Recording period	Data files acquired
09/08/06 - 23/08/06	20060809T150233Z_20060823T172756Z.ISAR5C_002 20060809T150233Z_20060823T172756Z.Wind 20060809T150233Z_20060823T172756Z.Vaisala 20060809T150233Z_20060823T172756Z.MPack 20060809T150233Z_20060823T172756Z.HTHERM
23/08/06 - 04/10/06	20060823T165821Z_20061004T200516Z.ISAR5C_002 20060823T165821Z_20061004T200516Z.Wind 20060823T165821Z_20061004T200516Z.Vaisala 20060823T165821Z_20061004T200516Z.MPack 20060823T165821Z_20061004T200516Z.HTHERM
04/10/06 - 19/10/06	20061004T202002Z_20061019T171810Z.ISAR5C_002 20061004T202002Z_20061019T171810Z.Wind 20061004T202002Z_20061019T171810Z.Vaisala 20061004T202002Z_20061019T171810Z.MPack 20061004T202002Z_20061019T171810Z.HTHERM
19/10/06 - 06/11/06	20061019T173521Z_20061106T185341Z.ISAR5C_002 20061019T173521Z_20061106T185341Z.Wind 20061019T173521Z_20061106T185341Z.Vaisala 20061019T173521Z_20061106T185341Z.MPack 20061019T173521Z_20061106T185341Z.HTHERM

B.4 Data records for D13: ISAR-003, 6 December 2006 to 4 January 2007

Recording period	Data files acquired
06/11/06 - 23/11/06	20061106T201005Z_20061123T163921Z.ISAR5C_003 20061106T201005Z_20061123T163921Z.Wind 20061106T201005Z_20061123T163921Z.Vaisala 20061106T201005Z_20061123T163921Z.MPack 20061106T201005Z_20061123T163921Z.HTHERM
23/11/06 - 30/11/06	20061123T161115Z_20061130T132207Z.ISAR5C_003 20061123T161115Z_20061130T132207Z.Wind 20061123T161115Z_20061130T132207Z.Vaisala 20061123T161115Z_20061130T132207Z.MPack 20061123T161115Z_20061130T132207Z.HTHERM
30/11/06 - 14/12/06	20061130T134635Z_20061214T140033Z.ISAR5C_003 20061130T134635Z_20061214T140033Z.Wind 20061130T134635Z_20061214T140033Z.Vaisala 20061130T134635Z_20061214T140033Z.MPack 20061130T134635Z_20061214T140033Z.HTHERM
14/12/06 - 04/01/07	20061214T140644Z_20070104T121557Z.ISAR5C_003 20061214T140644Z_20070104T121557Z.Wind 20061214T140644Z_20070104T121557Z.Vaisala 20061214T140644Z_20070104T121557Z.MPack 20061214T140644Z_20070104T121557Z.HTHERM

B.5 Data records for D14: ISAR-002, 8 February to 8 May 2007

Recording period	Data files acquired
08/02/07 - 02/03/07	20070208T131308Z_20070302T112600Z.ISAR5C_002 *No Wind data 20070208T131308Z_20070302T112600Z.Vaisala 20070208T131308Z_20070302T112600Z.MPack 20070208T131308Z_20070302T112600Z.HTHERM
02/03/07 - 06/03/07	20070302T123018Z_20070306T130045Z.ISAR5C_002 *No Wind data 20070302T123018Z_20070306T130045Z.Vaisala 20070302T123018Z_20070306T130045Z.MPack 20070302T123018Z_20070306T130045Z.HTHERM
06/03/07 - 12/03/07	20070306T131210Z_20070312T174221Z.ISAR5C_002 *No Wind data 20070306T131210Z_20070312T174221Z.Vaisala 20070306T131210Z_20070312T174221Z.MPack 20070306T131210Z_20070312T174221Z.HTHERM
12/03/07 - 16/03/07	20070312T174901Z_20070316T150907Z.ISAR5C_002 *No Wind data 20070312T174901Z_20070316T150907Z.Vaisala 20070312T174901Z_20070316T150907Z.MPack 20070312T174901Z_20070316T150907Z.HTHERM
16/03/07 - 20/03/07	20070316T163247Z_20070320T022407Z.ISAR5C_002 *No Wind data 20070316T163247Z_20070320T022407Z.Vaisala 20070316T163247Z_20070320T022407Z.MPack 20070316T163247Z_20070320T022407Z.HTHERM
20/03/07 - 23/03/07	20070320T022746Z_20070323T130145Z.ISAR5C_002 20070320T022746Z_20070323T130145Z.Wind 20070320T022746Z_20070323T130145Z.Vaisala 20070320T022746Z_20070323T130145Z.MPack 20070320T022746Z_20070323T130145Z.HTHERM
23/03/07 - 30/03/07	20070323T130708Z_20070330T142548Z.ISAR5C_002 20070323T130708Z_20070330T142548Z.Wind 20070323T130708Z_20070330T142548Z.Vaisala 20070323T130708Z_20070330T142548Z.MPack 20070323T130708Z_20070330T142548Z.HTHERM

Recording period	Data files acquired
30/03/07 - 08/05/07	20070330T154329Z_20070508T171839Z.ISAR5C_002 20070330T154329Z_20070508T171839Z.Wind 20070330T154329Z_20070508T171839Z.Vaisala 20070330T154329Z_20070508T171839Z.MPack 20070330T154329Z_20070508T171839Z.HTHERM

B.6 Data records for D15: ISAR-003, 8 May to 1 June 2007

Recording period	Data files acquired
08/05/07 - 01/06/07	20070508T171946Z_20070601T174704Z.ISAR5C_003 20070508T171946Z_20070601T174704Z.Wind 20070508T171946Z_20070601T174704Z.Vaisala 20070508T171946Z_20070601T174704Z.MPack 20070508T171946Z_20070601T174704Z.HTHERM

B.7 Data records for D16: ISAR-002, 4 June to 24 August 2007

Recording period	Data files acquired
04/06/07 - 19/06/07	20070604T170759Z_20070619T163537Z.ISAR5C_002 20070604T170759Z_20070619T163537Z.Wind 20070604T170759Z_20070619T163537Z.Vaisala 20070604T170759Z_20070619T163537Z.MPack 20070604T170759Z_20070619T163537Z.HTHERM
19/06/07 - 04/07/07	20070619T164200Z_20070704T182034Z.ISAR5C_002 20070619T164200Z_20070704T182034Z.Wind 20070619T164200Z_20070704T182034Z.Vaisala 20070619T164200Z_20070704T182034Z.MPack 20070619T164200Z_20070704T182034Z.HTHERM
04/07/07 - 10/07/07	20070704T184342Z_20070710T173938Z.ISAR5C_002 20070704T184342Z_20070710T173938Z.Wind 20070704T184342Z_20070710T173938Z.MPack 20070704T184342Z_20070710T173938Z.HTHERM
10/07/07 - 07/08/07	20070710T175359Z_20070807T152830Z.ISAR5C_002 20070710T175359Z_20070807T152830Z.Wind 20070710T175359Z_20070807T152830Z.MPack 20070710T175359Z_20070807T152830Z.HTHERM
07/08/07 - 24/08/07	No full resolution files were logged because of UPS failure

B.8 Data records for D17: ISAR-003, 24 August to 25 November 2007

Recording period	Data files acquired
24/08/07 - 27/08/07	20070824T185132Z_20070827T185503Z.ISAR5C_003 20070824T185132Z_20070827T185503Z.Wind 20070824T185132Z_20070827T185503Z.MPack 20070824T185132Z_20070827T185503Z.HTHERM
27/08/07 - 05/09/07	20070827T195449Z_20070905T162035Z.ISAR5C_003 20070827T195449Z_20070905T162035Z.Wind 20070827T195449Z_20070905T162035Z.MPack 20070827T195449Z_20070905T162035Z.HTHERM
05/09/07 - 02/10/07	20070905T170148Z_20071002T162928Z.ISAR5C_003 20070905T170148Z_20071002T162928Z.Wind 20070905T170148Z_20071002T162928Z.MPack 20070905T170148Z_20071002T162928Z.HTHERM
02/10/07 - 08/11/07	20071002T165329Z_20071108T131036Z.ISAR5C_003 20071002T165329Z_20071108T131036Z.Wind 20071002T165329Z_20071108T131036Z.MPack 20071002T165329Z_20071108T131036Z.HTHERM
08/11/07 - 20/11/07	20071108T141430Z_20071120T092522Z.ISAR5C_003 20071108T141430Z_20071120T092522Z.Wind 20071108T141430Z_20071120T092522Z.Vaisala 20071108T141430Z_20071120T092522Z.MPack 20071108T141430Z_20071120T092522Z.HTHERM
20/11/07 - 25/11/07	20071122T130720Z_20071125T035547Z.ISAR5C_003 20071122T130720Z_20071125T035547Z.Wind 20071122T130720Z_20071125T035547Z.MPack 20071122T130720Z_20071125T035547Z.HTHERM

B.9 Data records for D18: ISAR-003, 29 November 2007 to 7 January 2008

Recording period	Data files acquired
29/11/07 - 06/12/07	20071129T124448Z_20071206T142509Z.ISAR5C_003 20071129T124448Z_20071206T142509Z.Wind 20071129T124448Z_20071206T142509Z.MPack 20071129T124448Z_20071206T142509Z.HTHERM
06/12/07 - 18/12/07	20071206T142835Z_20071218T174837Z.ISAR5C_003 20071206T142835Z_20071218T174837Z.Wind 20071206T142835Z_20071218T174837Z.MPack 20071206T142835Z_20071218T174837Z.HTHERM
18/12/07 - 07/01/08	20071218T175907Z_20080107T140535Z.ISAR5C_003 20071218T175907Z_20080107T140535Z.Wind 20071218T175907Z_20080107T140535Z.MPack 20071218T175907Z_20080107T140535Z.HTHERM

Appendix C Intercomparison tests for CASOTS-2 Blackbody

An intercomparison test between CASOTS-2 and the NIST infrared calibration target was carried out at the Rosenstiel School for Marine and Atmospheric Science (RSMAS), University of Miami, USA from 12th March to 15th March 2006. The results of the comparisons were very promising and are shown in Figure C-1.

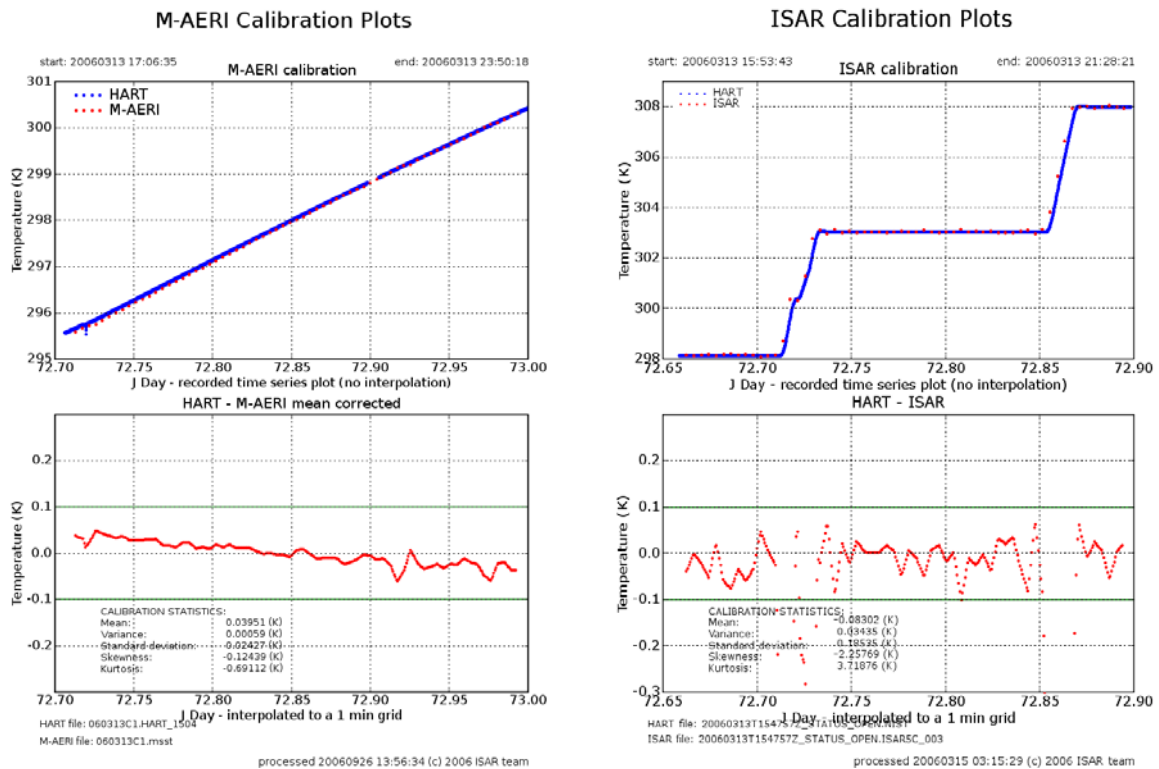


Figure C-1: (a) M-AERI - CASOTS-2 calibration curve (b) ISAR- NIST Calibration curve

The graph in Figure C-1 (a) shows the CASOTS-2 water bath temperature as measured by the HART thermometer (blue, top panel) compared to the temperature derived from the M-AERI measurements (red dots, top panel) and the difference between them in the bottom panel,

Figure C-1 (b) shows the water bath temperature of the NIST blackbody (blue top panel) compared to the temperature derived from ISAR-003 and the difference between the two measurements in the bottom panel.

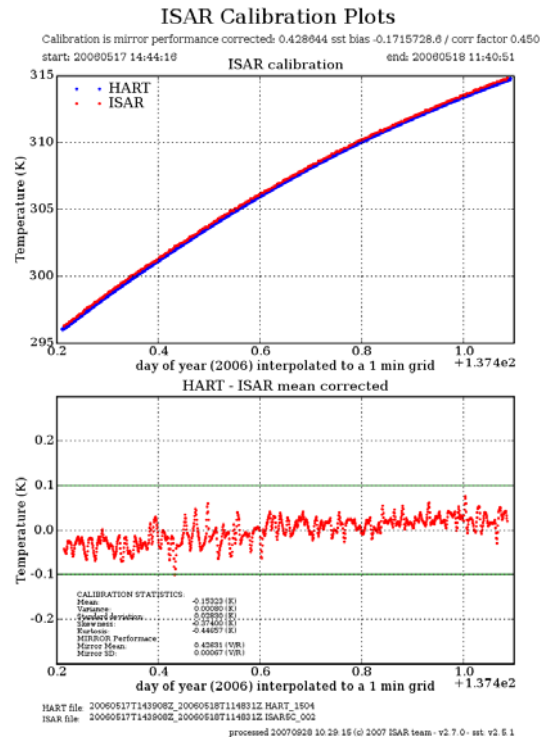
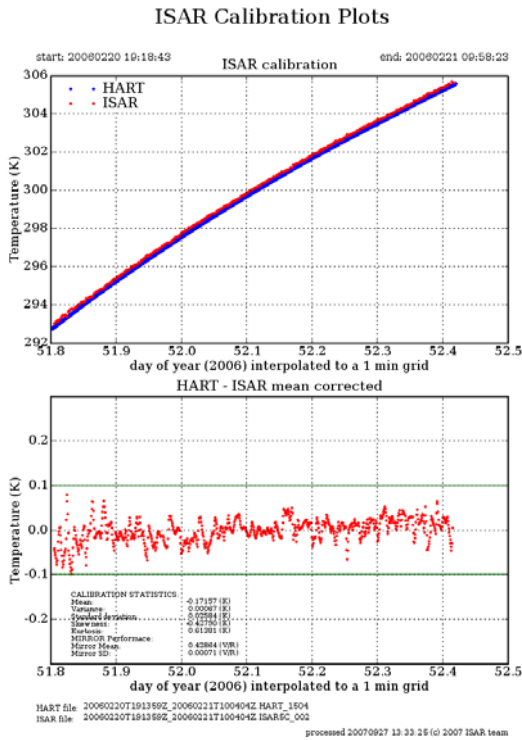
Even though the results shown here are very good, it was later discovered that the M-AERI instrument had used as a transfer standard between the RSMAS NIST blackbody and the CASOTS-2 blackbody that had a calibration error which could not be characterised. This means that we can only use the ISAR data in this comparison. However, using the ISAR instrument does only allow us to make some basic assumptions about the quality of the CASOTS-2 blackbody as the ISAR

instrument is a single channel instrument and the effective emissivity of the CASOTS-2 blackbody can not be estimated without the multi-channel measurement of the M-AERI instrument.

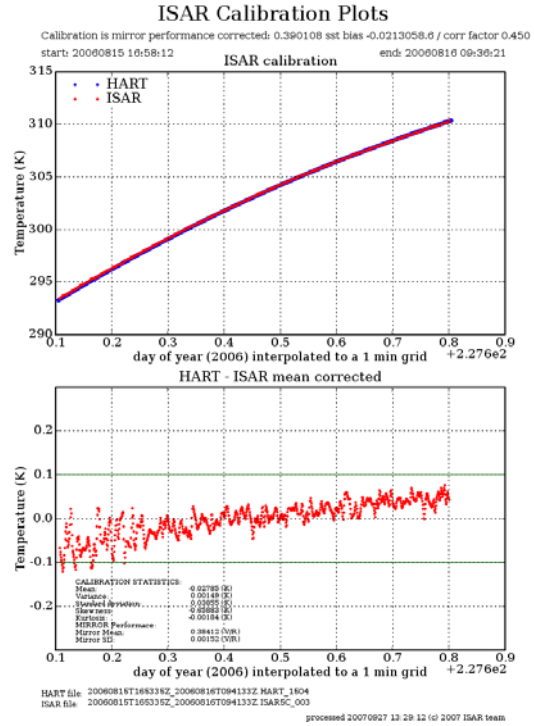
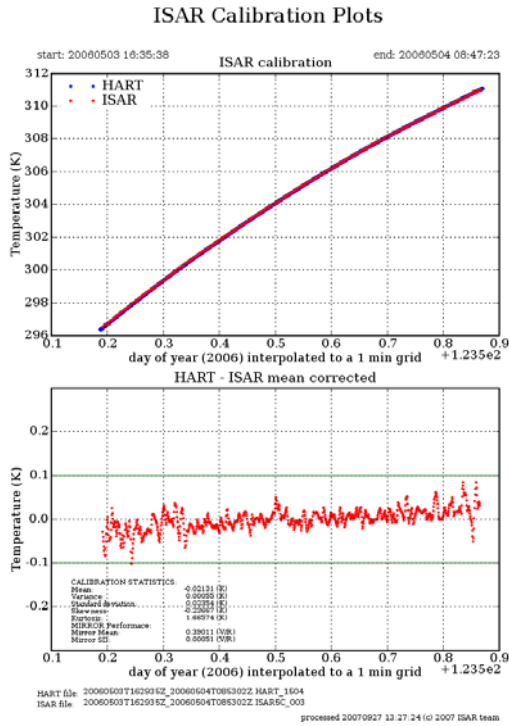
Using the ISAR instrument measurements, we can conclude that the CASOTS-2 blackbody does perform as well as the NIST blackbody in the measured temperature and spectral range, within the accuracy of the ISAR instrument. However we will need to perform another intercomparison experiment in the near future to firstly show that the CASOTS-2 blackbody performance has not changed over the years and secondly to measure the whole spectral range of the CASOTS-2 blackbody, not just the 9.6 to 11.5 μm range measured by the ISAR instrument.

Appendix D Pre and post cruise validation data

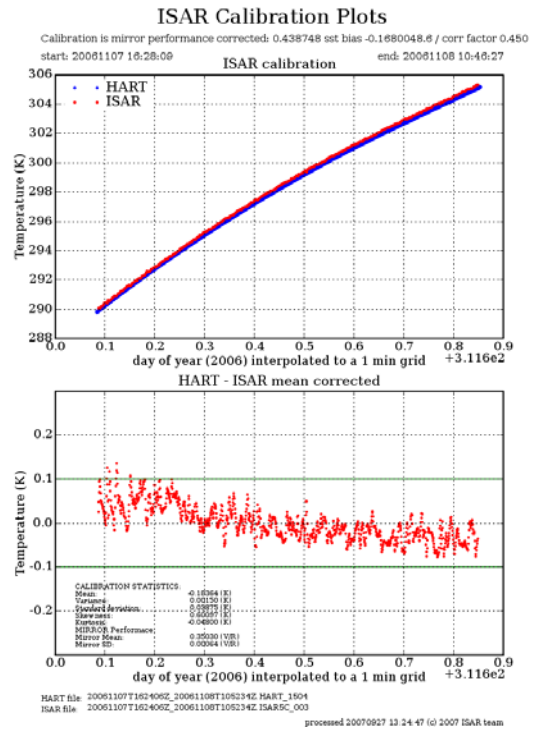
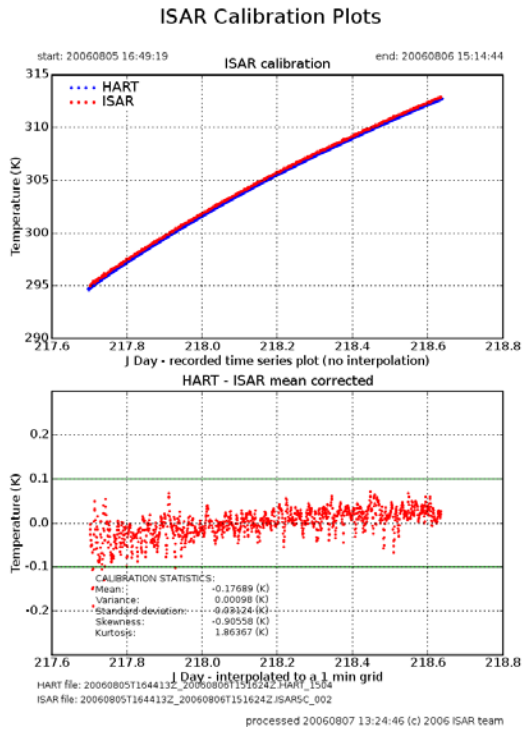
D.1 Calibration plots for D10: ISAR-002, 21 February to 10 May 2006



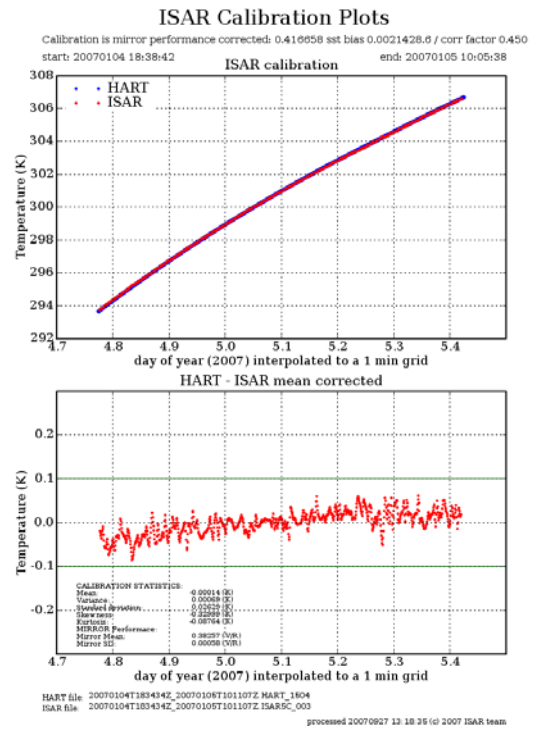
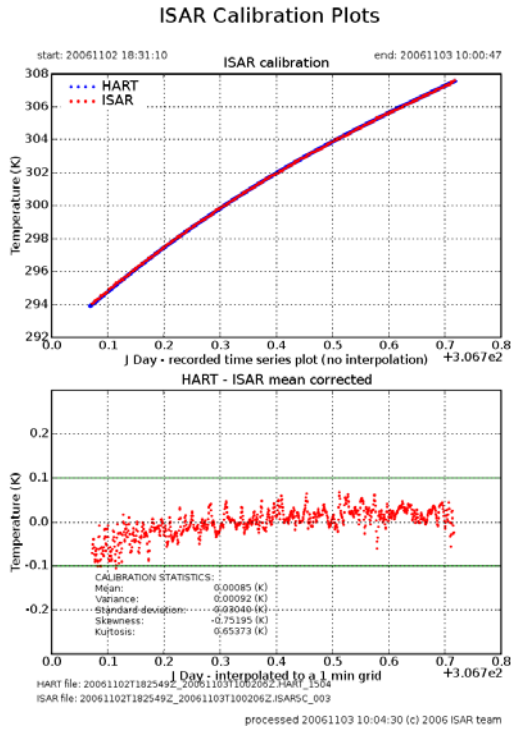
D.2 Calibration plots for D11: ISAR-003, 10 May to 9 August 2006



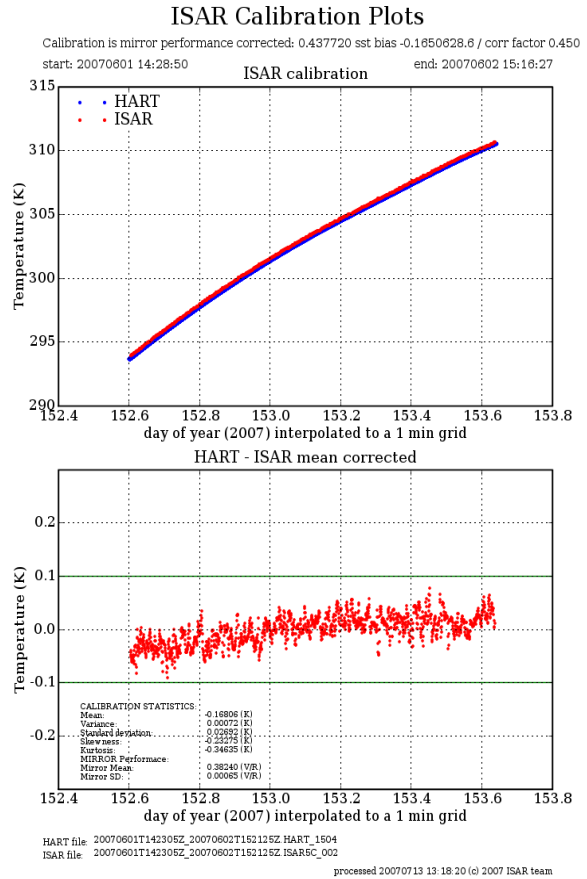
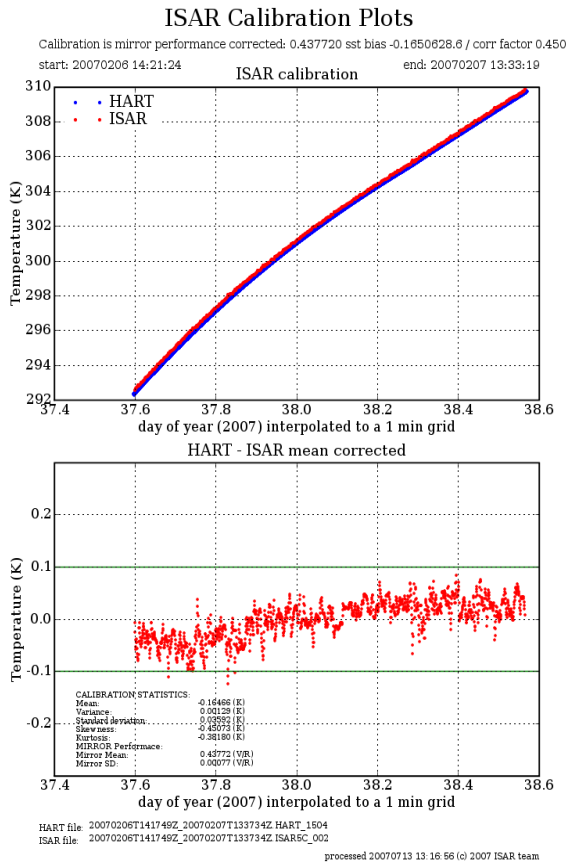
D.3 Calibration plots for D12: ISAR-002, 9 August to 6 November 2006



D.4 Calibration plots for D13: ISAR-003, 6 December 2006 to 4 January 2007



D.5 Calibration plots for D14: ISAR-002, 8 February to 8 May 2007

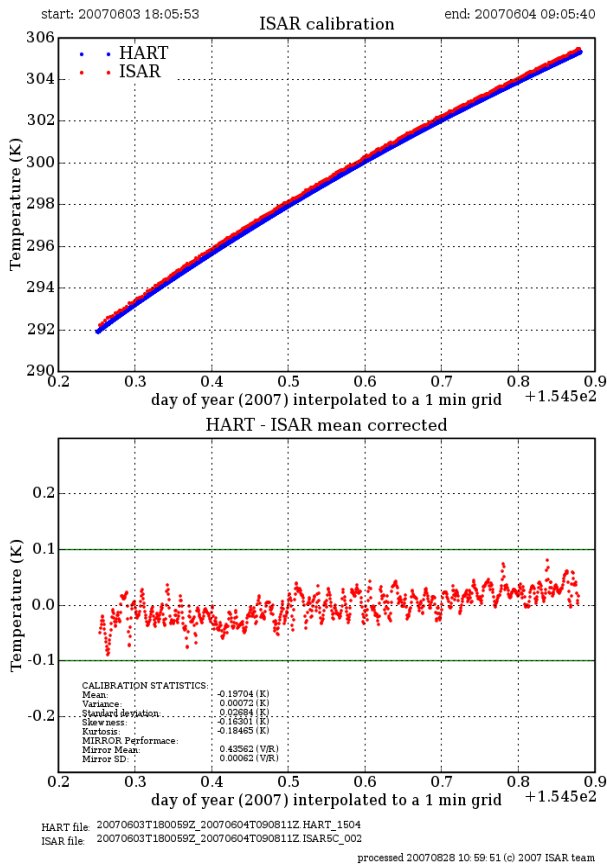


D.6 Calibration plots for D15: ISAR-002, 4 June to 24 August 2007

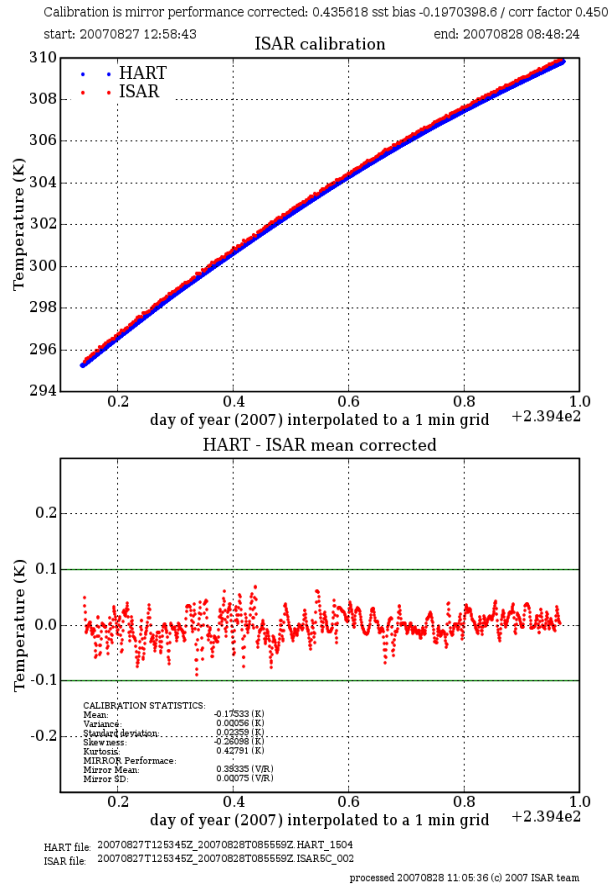
These plots are not included due to the failure of the scan drum during this deployment.

D.7 Calibration plots for D16: ISAR-002, 4 June to 24 August 2007

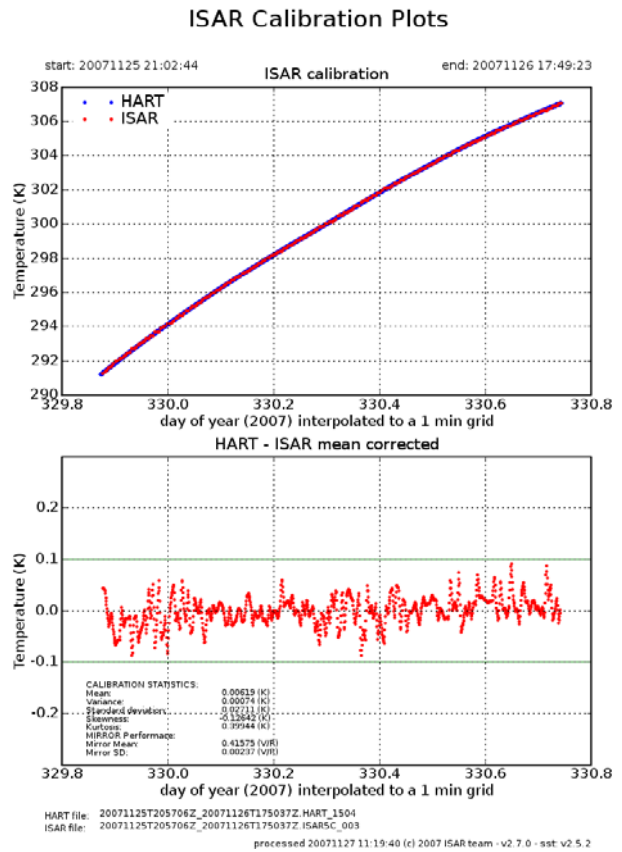
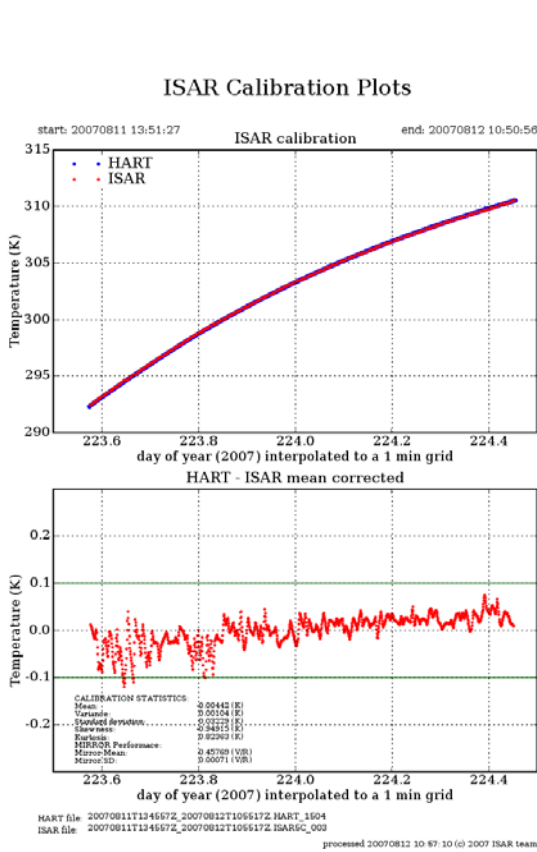
ISAR Calibration Plots



ISAR Calibration Plots

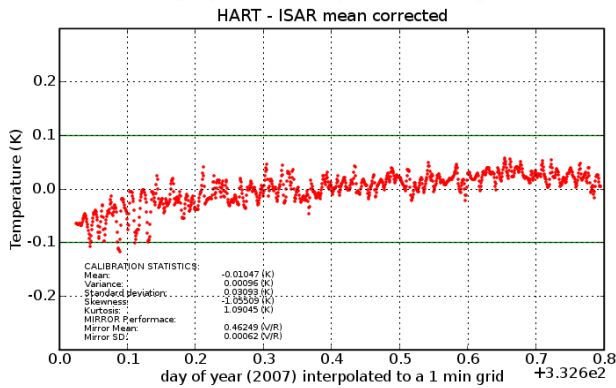
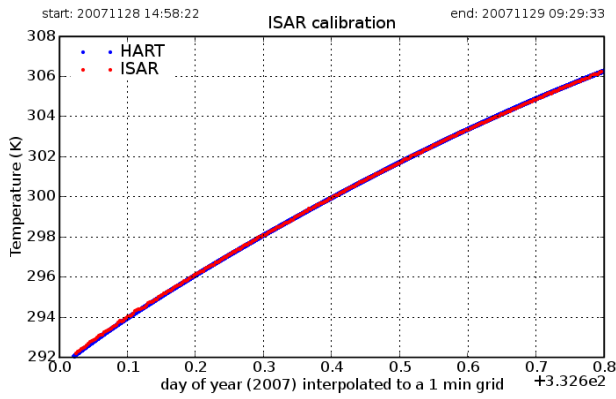


D.8 Calibration plots for D17: ISAR-003, 24 August to 25 November 2007



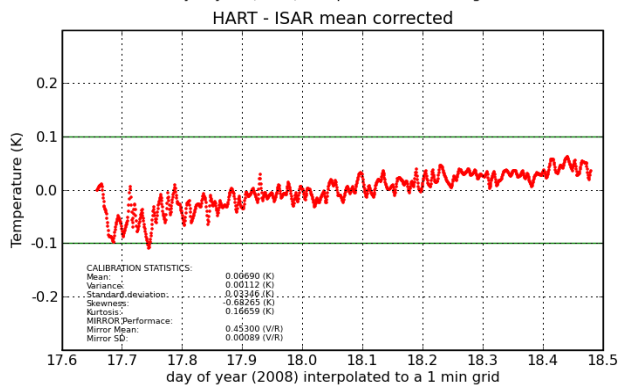
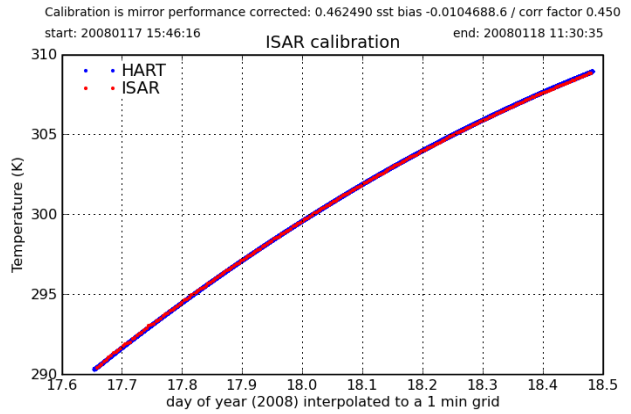
D.9 Calibration plots for D18: ISAR-003, 29 November 2007 to 7 January 2008

ISAR Calibration Plots



processed 20071129 09:40:52 (c) 2007 ISAR team - v2.7.0 - sst: v2.5.2

ISAR Calibration Plots



processed 20080118 12:17:31 (c) 2008 ISAR team - v2.7.0 - sst: v2.5.2

Appendix E ISAR Instrument Service Logs

ISAR 002	
01/02/06 - 19/02/06	Fitting of new mirror and performance tests
20/02/06 - 21/02/06	Pre-deployment calibration (D10)
21/02/06 - 10/05/06	Deployment on the <i>Pride of Bilbao</i> (D10)
11/05/06 - 13/05/06	Post-deployment calibration (D10)
20/05/06 - 01/06/06	Sensor inspection
02/06/06 - 10/06/06	Mirror change and testing
04/08/06 - 09/08/06	Pre-deployment calibration (D12)
09/08/06 - 06/11/06	Deployment on the <i>Pride of Bilbao</i> (D12)
07/11/06 - 12/11/06	Post-deployment calibration (D12)
13/11/06 - 31/12/06	Maintenance
01/01/07 - 28/01/07	Refitting and testing new mirror
29/01/07 - 03/02/07	Pre-deployment calibration (D14)
08/02/07 - 08/05/07	Deployment on the <i>Pride of Bilbao</i> (D14)
09/05/07 - 10/05/07	Post-deployment calibration (D14)
11/05/07 - 31/05/07	Maintenance
01/06/07 - 04/06/07	Pre-deployment calibration (D16)
04/06/07 - 24/08/07	Deployment on the <i>Pride of Bilbao</i> (D16)
25/08/07 - 31/08/07	Post-deployment calibration and maintenance (D16)
01/11/07 - 29/02/08	Electronics hardware upgrade

ISAR 003	
01/02/06 - 11/03/06	Maintenance and Software tests
12/03/06 - 17/03/06	Calibration and CASOTS 2 characterisation exercise at the University of Miami, Florida, USA
18/03/06 - 30/04/06	Maintenance and Software tests.
05/05/06 - 08/05/06	Pre-deployment calibration (D11)
10/05/06 - 09/08/06	Deployment on the <i>Pride of Bilbao</i> (D11)
09/08/06 - 16/08/06	Post deployment calibration (D11)
17/08/06 - 31/10/06	Maintenance
01/11/06 - 02/11/06	Fitting of new scan mirror (the old one had been used for a year and was approaching the end of its expected life).

ISAR 003	
03/11/06 - 05/11/06	Pre-deployment calibration (D13)
06/11/06 - 04/01/07	Deployment on the <i>Pride of Bilbao</i> (D13)
04/01/07 - 06/01/07	Post deployment calibration (D13)
06/02/07 - 06/04/07	Maintenance including mirror replacement
04/05/07 - 08/05/07	Pre-deployment calibration (D15)
08/05/07 - 01/06/07	Deployment on the <i>Pride of Bilbao</i> (D15) Fault discovered
01/06/07 - 04/06/07	Deployed but not operating on the <i>Pride of Bilbao</i> (D15)
04/06/07 - 30/06/07	Maintenance ⁵ and repair of scan drum problems
01/07/07 - 31/07/07	Scan drum tests
01/08/07 - 20/08/07	Endurance testing
21/08/07 - 24/08/07	Pre-deployment calibration (D17)
24/08/07 - 25/11/07	Deployment on the <i>Pride of Bilbao</i> (D17)
26/11/07 - 27/11/07	Post-deployment calibration (D17)
27/11/07 - 29/11/07	Repairs and maintenance
28/11/07 - 29/11/07	Pre-deployment calibration (D18)
29/11/07 - 07/01/08	Deployment on the <i>Pride of Bilbao</i> (D18)
07/01/08 - 20/01/08	Post-deployment calibration (D18)
20/01/08 - 31/01/08	Maintenance
06/02/08 - 07/02/08	Pre-deployment calibration (D19)
17/02/08 -	Deployment on the <i>Pride of Bilbao</i> (D19)

⁵ Note that, because of the scan drum failure on ISAR 003 during deployment D15, no post-deployment calibration could be performed. However after repairs and testing of the instrument a satisfactory calibration was performed.

Appendix F Acronyms

AATSR	Advanced Along-Track Scanning Radiometer
CASOTS	Combined Action for the Study of the Ocean Thermal Skin (EU)
Defra	Department for Environment, Food and Rural Affairs
GHRSSST-PP	GODAE High Resolution Sea Surface Temperature Pilot Project
GODAE	Global Ocean Data Assimilation Experiment
ISAR	Infrared SST Autonomous Radiometer
M-AERI	Marine-Atmosphere Emitted Radiance Interferometer
NIST	National Institute for Standards and Technology (USA)
NOCS	National Oceanography Centre, Southampton
PAR	Photosynthetically Available radiation
PIR	Precision Infrared Radiometer
RSMAS	Rosentiel School of Marine and Atmospheric Science (USA)
SST	Sea Surface Temperature